


12-2021

Data Analytics for Sustainable Food and Agriculture Systems

Megan Lord Reavis
University of Arkansas, Fayetteville

Follow this and additional works at: <https://scholarworks.uark.edu/etd>

 Part of the [Agricultural Economics Commons](#), [Climate Commons](#), [Food Chemistry Commons](#), [Food Processing Commons](#), [Natural Resources and Conservation Commons](#), [Sustainability Commons](#), and the [Water Resource Management Commons](#)

Citation

Reavis, M. L. (2021). Data Analytics for Sustainable Food and Agriculture Systems. *Graduate Theses and Dissertations* Retrieved from <https://scholarworks.uark.edu/etd/4270>

This Dissertation is brought to you for free and open access by ScholarWorks@UARK. It has been accepted for inclusion in Graduate Theses and Dissertations by an authorized administrator of ScholarWorks@UARK. For more information, please contact scholar@uark.edu, uarepos@uark.edu.

Data Analytics for Sustainable Food and Agriculture Systems

A dissertation submitted in partial fulfillment
of the requirements for the degree of
Doctor of Philosophy in Biological Sciences

by

Megan Lord Reavis
North Carolina State University
Bachelor of Science in Animal Science, 2015
University of Arkansas
Master of Science in Crop, Soil, and Environmental Science, 2017

December 2021
University of Arkansas

This dissertation is approved for recommendation to the Graduate Council.

Kusum Naithani, Ph.D.
Dissertation Director

Larry Purcell, Ph.D.
Committee Member

Andy Pereira, Ph.D.
Committee Member

James Coleman, Ph.D.
Committee Member

ABSTRACT

The increasing concentration of anthropogenic greenhouse gases in the atmosphere is altering the climate, posing a serious threat to global agriculture and food security. Agriculture and food production contribute a quarter of all GHG emissions produced, so there is a critical need to limit emissions in this area while increasing food production to feed the anticipated 10 billion people by 2050. To address the needs of the future, data-driven solutions are needed to guide decision-making and provide support for actionable climate mitigation and survival strategies. Research efforts must be focused on analyzing problems on multiple scales, identifying new ways to answer relevant questions, and translating available data into useful solutions.

This dissertation examines three diverse areas of research with an overarching goal of supporting sustainable food and agriculture future through developing data analytics tools. The first chapter evaluated the public GHG emission disclosure practices and climate goals of the top 100 global food and beverage companies, the second chapter developed a novel mechanistic model in a probabilistic framework to quantify and predict photosynthesis response to drought to support crop phenotyping, and the third chapter parameterized a common phenotyping model in a probabilistic framework to understand phenotypic plasticity of a major cereal crop of the world.

The first chapter highlights the gap in current GHG reporting practices of the largest food and beverage companies in the world. Roughly a third of companies assessed had some sort of climate goal, though the ability of those goals to significantly reduce global climate emissions is negligible in the majority of cases. Many companies lack any sort of public disclosure as well, and companies that fail to measure emissions are unable to set reduction goals. There is a

significant disconnect between what is needed to keep global warming under 1.5 °C and the action currently being taken to do so.

The second chapter describes a novel multilevel Bayesian drought response curve model based on Michaelis-Menten equation for phenotyping drought sensitivity in rice genotypes. The model was successfully implemented in eight rice genotypes and drought sensitivity ranking was validated using yield data from the field.

The third chapter highlights the need to understand the plastic nature of plants and tested a fast non-sequential photosynthesis light response curve model in field condition. The growing environment of the rice plants in this research significantly altered their maximum photosynthesis rate, and the method of generating such curves was less important than the environment.

© 2021 by Megan Lord Reavis
All Rights Reserved

ACKNOWLEDGMENTS

I could not have completed this dissertation or made it through the last four years without the amazing support of many people. First, I would like to thank my committee who graciously guided this research: Kusum Naithani, Larry Purcell, Andy Pereira, and Jim Coleman. I owe so much to my phenomenal advisor, Kusum Naithani. Her unwavering confidence in me and this work was invaluable to me during the hardest parts of the writing process. She encouraged me and fought for me, and I am so grateful and honored to have been her student. Thank you to the Pereira lab — Anuj Kumar and Julie Thomas — whose guidance and assistance setting up the drought experiments was so appreciated. Thank you to Sara Yingling who so generously helped get my field experiments up and running and who braved the spiders to help me harvest my plants, and thank you to Ashley Kiersey who cheerfully counted seemingly endless grains of rice. I am so thankful to the Purcell lab — Marilyn Davis, Andy King, and Caio dos Santos — for their help with my growth chamber experiments as well. I could not have done this research without their help.

I would like to thank Jenny Ahlen and Joe Rudek for their mentorship during my internship at the Environmental Defense Fund and for their guidance on the greenhouse gas emissions chapter. They both modeled what careers in sustainability could look like, and the work they do continues to inspire me.

Thank you to Renee Sniegocki who made us coffee each morning in the lab and who made me laugh when things felt hard, to Ayanna St. Rose who spent months in a rice paddy with me in the middle of the summer, and to the rest of the lab whose friendship and encouragement along the way has been so cheering: Alexis O'Callahan, Yang Kai Tang, and Eston Dunn.

To my parents, sister, and brother, and to my rock-solid community of friends, thank you for your never-ending support and love, which made this journey an enjoyable one. And thank you to my wonderful husband who has walked this grad school path with me every step of the way; I wouldn't have wanted to do it with anyone else.

TABLE OF CONTENTS

<i>INTRODUCTION</i>	1
REFERENCES	3
<i>CHAPTER 1: Evaluation of greenhouse gas emissions and climate mitigation goals of the global food and beverage sector</i>	5
ABSTRACT	5
1. INTRODUCTION	6
2. METHODS	8
2.1 Food and Beverage Company Selection.....	8
2.2 Data Collection	8
2.3 Understanding Emissions and Targets	9
2.4 Target Evaluation	11
3. RESULTS AND DISCUSSION	13
3.1 Extent of Publicly Disclosed GHG Emissions and Climate Goals	13
3.2 Areas for Improvement in Publicly Disclosed GHG Emissions and Climate Goals.....	18
4. CONCLUSIONS.....	24
5. REFERENCES	25
SUPPLEMENTARY INFORMATION.....	29
<i>CHAPTER 2: Drought Response Curve: A Novel Mechanistic Method for Quantifying Phenotypic Expression of Drought Sensitivity in Crops</i>	35
ABSTRACT	35

1. INTRODUCTION	36
2. MATERIALS AND METHOD.....	39
2.1 Plant Material	39
2.2 Growing Conditions	40
2.3 Harvesting and Yield Evaluation.....	43
2.4 Statistical Analysis	43
3. RESULTS	45
3.1 Model Goodness-of-Fit.....	45
3.2 Developing a mechanistic model for photosynthesis response to drought.....	46
3.3 Effect of growing conditions on photosynthesis response to drought.....	47
3.4 Genotypic differences in photosynthesis response to drought	49
4. DISCUSSION	50
5. CONCLUSIONS.....	53
6. REFERENCES	54
 <i>CHAPTER 3: Effects of Growing Conditions and Measurement Methods on Phenotypic</i>	
<i>Expression of Photosynthesis.....</i>	<i>60</i>
ABSTRACT	60
1. INTRODUCTION	61
2. METHODS	64
2.1 Plant Material	64
2.2 Photosynthesis Light Response Curve Measurements	64
2.3 Statistical Analysis	67

3. RESULTS	70
3.1 Model Goodness-of-Fit.....	70
3.2 Effect of Growing Conditions on Phenotypic Expression of Photosynthesis	70
3.3 Effect of Measurement Methods on Phenotypic Expression of Photosynthesis	71
4. DISCUSSION	73
4.1 Effect of Growing Conditions on Phenotypic Expression of Photosynthesis	73
4.2 Effect of Measurement Methods on Phenotypic Expression of Photosynthesis	74
5. CONCLUSIONS.....	75
6. REFERENCES	75
APPENDIX 1	80
<i>CONCLUSION</i>	94
APPENDIX 2	96

LIST OF TABLES

Chapter 1

Table 1. Breakdown of CDP scores of those 61 companies with available scores.....16

Supplementary Table S1. Information on all companies used in this study. Companies listed alphabetically that were used in this study, along with where data for each company was obtained, the company headquarters, and the ranking of each company on Food Engineering's top 100 list [#]. Data was primarily obtained from CDP reports (which can be found by searching the company on CDP's website: <https://www.cdp.net/en/scores>), the Science Based Targets Initiative (SBTi, which can be found on their website: <https://sciencebasedtargets.org/companies-taking-action>), or company websites (given in table)29

Chapter 2

Table 1. Description of selected rice genotype and their drought sensitivity.....40

Chapter 3

Table 1. Information about rice genotypes used across different growing environments: F = field, GC = growth chamber, GH = greenhouse. Sequential and non-sequential light response curves were conducted on all genotypes.....64

Table A1. Summary statistics for genotype-level parameters in field including A_{max} (maximum rate of photosynthesis), Rd (mitochondrial respiration), α (apparent quantum efficiency of photosynthesis), and θ (curvature shape parameter). [1] = 310588, [2] = 310723, [3] = 311644, [4] = 311677, [5] = 311795, [6] = Nagina 22, [7] = Zhe733. D is the sum of the squared deviation and SD is the standard deviation of modeled observations.....80

Table A2. Summary statistics for plant-level and genotype-level parameters in growth chamber including A_{max} (maximum rate of photosynthesis), Rd (mitochondrial respiration), α (apparent quantum efficiency of photosynthesis), and θ (curvature shape parameter). [1] = 310588, [2] = 310723, [3] = 311644, [4] = 311677, [5] = 311795, [6] = Nagina 22, [7] = Zhe733. D is the sum of the squared deviation and SD is the standard deviation of modeled observations.....82

Table A3. Summary statistics for plant-level and genotype-level parameters in greenhouse including A_{max} (maximum rate of photosynthesis), Rd (mitochondrial respiration), α (apparent quantum efficiency of photosynthesis), and θ (curvature shape parameter). [1] = 310588, [2] = 310723, [3] = 311644, [4] = 311677, [5] = 311795, [6] = Nagina 22, [7] = Zhe733. D is the sum of the squared deviation and SD is the standard deviation of modeled observations.....90

LIST OF FIGURES

Chapter 1

Figure 1. Distribution of scope 1, 2, and 3 emissions	10
Figure 2. Heat map of company emission and goal disclosure.....	15
Figure 3. Distribution of absolute and intensity climate goals across scopes.....	17
Figure 4. Base, current, and target year scope 1, 2, and 3 emissions for 17 companies.....	19
Figure 5. Base, current, and target year scope 1 and 2 emissions for 27 companies.....	21

Chapter 2

Figure 1. Experimental setup for (a) field and (b) growth chamber. The timelines display significant events throughout the two experiments in days after planting seeds. The growth chamber experiment was completed in 3 rounds, so R1, R2, and R3 refer to rounds 1, 2, and 3, respectively.....	39
Figure 2. Relationship between observed and modeled values of the net photosynthesis rate (A_N , $\mu\text{mol m}^{-2} \text{s}^{-1}$) showing the model goodness-of-fit across growing environments. Error bars represent 2.5% (bottom) and 97.5% (top) credible intervals. The dotted line represents 1:1 line and the solid black line represents the linear fit to the data.....	45
Figure 3. Photosynthesis (A_N , $\mu\text{mol m}^{-2} \text{s}^{-1}$) response to changing soil moisture in 310588 (a) 310723 (b), and 311795 (c). Purple line is the model fit ($A_N=A_{max}\theta/(PLA_{50} + \theta)$, where A_{max} is maximum photosynthesis ($\mu\text{mol m}^{-2} \text{s}^{-1}$), and θ is volumetric soil moisture (%)) to the observed data (purple circles).....	46
Figure 4. Photosynthetic drought response curves (a,d,g,j,m,p) and posterior density distribution of photosynthesis model parameters A_{max} ($\mu\text{mol m}^{-2} \text{s}^{-1}$) and PLA_{50} (%) for six rice (<i>Oryza sativa</i>) genotypes under field (green) and growth chamber (pink) conditions. Green and pink lines are the fit of a Michaelis-Menten model ($A_N=A_{max}*\theta/(PLA_{50} + \theta)$, where A_{max} is maximum photosynthesis ($\mu\text{mol m}^{-2} \text{s}^{-1}$), θ is volumetric soil moisture (%), and PLA_{50} is θ at 50% of A_{max}) for field and growth chamber plants, respectively.....	48
Figure 5. Posterior probability distributions for PLA_{50} (%) and A_{max} ($\mu\text{mol m}^{-2} \text{s}^{-1}$) of each genotype.....	49
Figure 6. Relationship between the PLA_{50} (%) and A_{max} ($\mu\text{mol m}^{-2} \text{s}^{-1}$) model parameters of field and growth chamber plants and mean number of filled grains per panicle of field plants. Error bars are standard error about the mean.....	50

Figure 7. Drought sensitivity ranking of the eight genotypes selected for this work based on the multilevel Bayesian drought response curve model.....52

Chapter 3

Figure 1. Images showing measurements of rice plants with the LI-6400XT across different growing environments including (a) field, (b) growth chamber-grown pots acclimated to field conditions, and (c) greenhouse conditions.....66

Figure 2. Relationship between observed and modeled values of the net photosynthesis rate (A_N , $\mu\text{mol m}^{-2} \text{s}^{-1}$) showing the model goodness-of-fit across different growing environments. Error bars represent 2.5% (bottom) and 97.5% (top) credible intervals. The dotted line represents 1:1 line and the solid black line represents the linear fit to the data.....69

Figure 3. Photosynthesis light response curves (a, f, k) and posterior density distribution of photosynthesis model parameters α ($\mu\text{mol m}^{-2} \text{s}^{-1}$), A_{max} ($\mu\text{mol m}^{-2} \text{s}^{-1}$), R_d ($\mu\text{mol m}^{-2} \text{s}^{-1}$), and θ for three rice (*Oryza sativa*) genotypes under field (green), growth chamber (pink), and greenhouse (blue) conditions. Green, pink, and blue lines are the fit of a non-rectangular hyperbola model for field, growth chamber, and greenhouse plants, respectively.....71

Figure 4. Photosynthetic light response curves (a, f, k, p) and photosynthetic model parameters α (b, g, l, q), A_{max} (c, h, m, r), R_d (d, i, n, s), and θ (e, j, o, t) for four rice (*Oryza sativa*) genotypes under field (green) and growth chamber (pink) conditions. Green and pink lines are the fit of a non-rectangular hyperbola model for field and growth chamber plants, respectively.....72

LIST OF PUBLISHED PAPERS

Chapter 1 is accepted for publication in the journal *Frontiers in Sustainable Food Systems*.

Reavis, M., Ahlen, J., Rudek, J., Naithani, K. 2021. Evaluation of greenhouse gas emissions and climate mitigation goals of the global food and beverage sector. *Frontiers in Sustainable Food Systems*.

INTRODUCTION

World food security is a pressing concern as the population grows and the warming climate threatens food production (Kissoudis et al., 2016; Searchinger et al., 2019). Feeding 10 billion people by 2050 will require closing a food gap of 56% while emitting less greenhouse gases (GHGs) and using 593 million-fewer hectares of land to do so (Searchinger et al., 2019). There is a critical need to increase the resource efficiency of agriculture — producing more food per hectare, per kilogram of fertilizer, and per liter of water — to create a sustainable food future (Khush, 2005; Searchinger et al., 2019).

Food production accounts for 25% of the global GHG emissions (GRAIN, 2018; Ritchie, 2019; Searchinger et al., 2019). Land use change for cropland and pastureland, methane from livestock, and inefficient on-farm practices contribute millions of tons of CO₂ to the atmosphere every year (IPCC, 2014). Increasing global temperature and decreasing water availability are putting agriculture and food production systems at risk around the world, and these patterns will likely get worse if anthropogenic emissions are not significantly reduced.

Over the past 10,000 years, atmospheric CO₂ concentrations have remained fairly constant around 300-310 ppm, yet since the Industrial Revolution, anthropogenically-produced GHGs have been steadily rising (IPCC, 2014). The last three decades have each been successively warmer than any previous decade since 1950. Atmospheric CO₂ concentrations are currently 415 ppm (NOAA, 2021), more than 100 ppm greater than they have been for millennia (NASA, 2021). The increased concentration of GHGs in the atmosphere is universally accepted as the driving cause of climate warming (Forster et al., 2007; IPCC, 2018). The increase and severity of extreme weather events due to the changing climate will have greater consequences for agriculture than the changing climate alone (Easterling et al., 2007).

The following chapters in this dissertation focus on developing data analytics tools to support sustainable food and agriculture systems. The first chapter evaluates GHG emissions reporting from the top 100 global food and beverage companies. Continued increase in global GHG emissions for food production poses a serious risk to the current climate and future capacities for food production as well. Large food and beverage companies are responsible for massive emissions (GRAIN 2018), and, being such a significant source, have the grand opportunity to drastically cut emissions to keep climate warming to no more than 1.5 °C. We developed a data analytic tool to evaluate GHG emissions and climate goals of the top 100 global food and beverage companies using publicly available data. This chapter has been accepted in the journal *Frontiers in Sustainable Food Systems* to be published in 2022.

The second chapter describes a novel multilevel Bayesian drought response curve model based on Michaelis-Menten equation for phenotyping drought sensitivity in rice genotypes. The model was successfully implemented in eight rice genotypes and drought sensitivity ranking was validated using yield data from the field.

The third chapter highlights the need to understand the degree of phenotypic plasticity of plants and tested a fast non-sequential photosynthesis light response curve model in field condition. The growing environment of the rice plants in this research significantly altered their maximum photosynthesis rate, and the method of generating such curves was less important than the environment.

Across all chapters, the main focus is on developing data analytics tools for supporting sustainable food and agriculture production systems. The challenge over the next 30 years will be to understand the gaps in our knowledge and begin to rapidly develop solutions. GHG emissions from the food and agriculture sector are a significant portion of the anthropogenic

emissions globally, and there is an urgent need to develop solutions for increasing productivity while reducing GHG emissions to ensure global food security.

REFERENCES

- Easterling, W., Aggarwal, P., Batima, P., Brander, K., Erda, L., Howden, M., et al. (2007). Food, fibre and forest products. Cambridge, UK: Cambridge University Press.
- Forster, P., Ramaswamy, V., Artaxo, P., Bernsten, T., Betts, R., Fahey, D. W., et al. (2007). Changes in Atmospheric Constituents and in Radiative Forcing. 106.
- GRAIN (2018). Emissions impossible: How big meat and dairy are heating up the planet. Available at: <https://grain.org/article/entries/5976-emissions-impossible-how-big-meat-and-dairy-are-heating-up-the-planet> [Accessed April 21, 2021].
- IPCC (2014). Climate Change 2014: Synthesis Report. Contribution of Working Groups I, II and III to the Fifth Assessment Report of the Intergovernmental Panel on Climate Change [Core Writing Team, R.K. Pachauri and L.A. Meyer (eds.)]. IPCC, Geneva, Switzerland, 151 pp.
- IPCC (2018). Global warming of 1.5°C. An IPCC Special Report on the impacts of global warming of 1.5°C above pre-industrial levels and related global greenhouse gas emission pathways, in the context of strengthening the global response to the threat of climate change. Available at: https://www.ipcc.ch/site/assets/uploads/sites/2/2019/05/SR15_SPM_version_report_LR.pdf [Accessed June 4, 2021].
- Khush, G. S. (2005). What it will take to Feed 5.0 Billion Rice consumers in 2030. *Plant Mol Biol* 59, 1–6. doi:10.1007/s11103-005-2159-5.
- Kissoudis, C., van de Wiel, C., Visser, R. G., and van der Linden, G. (2016). Future-proof crops: challenges and strategies for climate resilience improvement. *Current Opinion in Plant Biology* 30, 47–56. doi:10.1016/j.pbi.2016.01.005.
- NASA (2021). Graphic: The relentless rise of carbon dioxide. *Climate Change: Vital Signs of the Planet*. Available at: https://climate.nasa.gov/climate_resources/24/graphic-the-relentless-rise-of-carbon-dioxide [Accessed November 12, 2021].
- NOAA (2021). Global Monitoring Laboratory - Carbon Cycle Greenhouse Gases. Available at: <https://gml.noaa.gov/ccgg/trends/monthly.html> [Accessed November 12, 2021].
- Ritchie, H. (2019). Food production is responsible for one-quarter of the world's greenhouse gas emissions. *Our World in Data*. Available at: <https://ourworldindata.org/food-ghg-emissions> [Accessed February 12, 2021].

Searchinger, T., Waite, R., Hanson, C., and Ranganathan, J. (2019). Creating a sustainable food future: a menu of solutions to feed nearly 10 billion people by 2050. World Resources Institute Available at: https://research.wri.org/sites/default/files/2019-07/WRR_Food_Full_Report_0.pdf [Accessed February 12, 2021].

CHAPTER 1: Evaluation of greenhouse gas emissions and climate mitigation goals of the global food and beverage sector

Co-authors: Kusum Naithani, Jenny Ahlen, Joe Rudek

ABSTRACT

The dramatic increase of emitted greenhouse gases (GHGs) by humans over the past century and a half has created an urgency for monitoring, reporting, and verifying GHG emissions as a first step towards mitigating the effects of climate change. Fifteen percent of global GHG emissions come from agriculture, and companies in the food and beverage industry are starting to set climate goals. We examined the GHG emissions reporting practices and climate goals of the top 100 global food and beverage companies and determined whether their goals are aligned with the science of keeping climate warming well below a 2 °C increase. Using publicly disclosed data in CDP Climate reports and company sustainability reports, we found that over two thirds of the top 100 (as ranked by Food Engineering) global food and beverage companies disclose at least part of their total company emissions and set some sort of climate goal that includes scope 1 and 2 emissions. However, only about half have measured, disclosed, and set targets for scope 3 emissions, which often encompass more than 87% of a company's emissions across the entire value chain. We also determined that companies, despite setting scope 1, 2, and 3 targets, may be missing the mark on whether their targets are significantly reducing global emissions. Our results present the current disclosure and emission goals of the largest food and beverage companies and highlight an urgent need to begin and continue to set truly ambitious, science-aligned climate goals.

1. INTRODUCTION

Since the start of the first Industrial Revolution around 1760, human activities have emitted greenhouse gases (GHGs) in excess of those emitted by natural sources. The rise in GHG concentration in the atmosphere over the years has steadily warmed the planet, leading to a rise in the global surface temperature (IPCC 2021). One such shift in the global climate in the 1980s drew the concern of scientists and the public to the increasing atmospheric GHGs (Reid et al. 2016). In 1990, a report by the Stockholm Environmental Institute declared an increase of 2 °C above pre-industrial times to be the global temperature limit, and going beyond that limit may result in “grave damage to ecosystems” (Rijsberman and Swart 1990). Twenty-five years later, 196 countries signed the Paris Climate Agreement, agreeing to limit global warming to well below 2 °C, preferably below 1.5 °C. This is a difficult task, however, as it calls for a massive shift in the way we currently do things and will require aggressive climate action from large emitters.

The global food and beverage sector is one significant source of GHG emissions. Food production accounts for roughly a quarter of the anthropogenic GHGs emitted annually across the globe, (Ritchie 2019) and the sector as a whole accounts for roughly a third of global emissions (Crippa et al. 2021). Significant reductions in global GHG emissions are not possible without reductions from the food and beverage industry (Kobayashi and Richards 2021). The majority of emissions come from the supply chains of food and beverage companies, so setting climate goals to reduce the emissions within a company’s value chain is of the utmost importance (Kobayashi and Richards 2021).

Climate targets that align with the goals of the Paris Climate Agreement and a net-zero future are considered science-based (SBTi 2021b). The Science Based Targets initiative

(<https://sciencebasedtargets.org/>) is a framework that helps companies set targets grounded, first and foremost, in science. As scientists (Ripple et al. 2019), consumers (Lai and Schiano 2021), and employees (Sax 2020) are increasingly calling for more direct and aggressive climate action from large corporations, more companies are getting on board (Winston 2017, NewClimate Institute and Data-Driven EnvironLab 2020). In 2016, 119 companies had set targets with the Science Based Targets initiative (SBTi) (Faria 2016), and currently, over 1700 companies have committed or set climate goals with SBTi (SBTi 2021a). However, previous studies have shown that while climate policy has improved over the years, and more countries and individual companies have set emission reduction goals, there has been no significant decrease in global emissions (Haffar and Searcy 2018, Christensen and Olhoff 2019).

So, a third of the global anthropogenic GHG emissions come from food and beverage company activities, and as the population grows, demand for food will only increase (Gerber et al. 2013), resulting in greater GHG emissions (Searchinger et al. 2019). As large emitters (GRAIN 2018), setting climate targets is important for food and beverage companies and requires them to inventory their emissions. However, emissions across the entire value chain must be accounted for and included in emission targets. It is unclear how many large food and beverage companies are setting climate goals to reduce their total value chain emissions and how significant their current and potential reductions may be on global atmospheric GHG concentrations. In this research, we evaluate the GHG emissions reporting practices of the top 100 (ranked by Food Engineering) global food and beverage companies with the specific goals of (1) demonstrating the extent of publicly disclosed GHG emissions and climate goals, and (2) identifying areas for improvement in publicly disclosed GHG emissions and climate goals in

order to continue making significant progress towards reducing global GHG emission and warming.

2. METHODS

2.1 Food and Beverage Company Selection

To study the GHG emissions and goals across the food and beverage industry, we selected the top 100 global food and beverage companies as ranked by Food Engineering (Food Engineering 2020). The food sales of these 100 companies make up roughly 15% of the food and agriculture industry worldwide (Plunkett Research, Ltd. 2021). Company size was based on revenue generated from food sales only, not overall revenue. For example, Cargill (ranked 9th on the list) has a greater overall yearly revenue than Nestle (ranked 1st on the list), but Cargill's revenue from food sales alone was less than Nestle's because Cargill sells other agricultural products besides food, thus their lower ranking. The selected companies operate all over the world and consist of both food and beverage (alcoholic and nonalcoholic) processors and manufacturers. The companies, their industry, and headquarters are summarized in Supplementary Table 1.

2.2 Data Collection

We primarily use resources from the Science Based Target Initiative (SBTi) and CDP (formerly Carbon Disclosure Project), two organizations that guide companies toward greater climate action. The SBTi is a collaboration between CDP, the United Nations Global Compact, the World Resources Institute, and WWF (World Wildlife Fund). They aim to fight climate change by providing companies with technical assistance and resources to set climate goals

aligned with science. Science-based targets are goals aligned with keeping global temperature rise to well below 2 °C above pre-industrial levels. Companies set climate targets, and approval is based on rigorous SBTi criteria. We recorded the goals of the companies that had SBTi-approved climate goals.

CDP (<https://www.cdp.net/en>) is a global non-profit organization that works to make environmental reporting the norm by helping companies, cities, and states measure, report, and manage risk in areas of climate, water security, and deforestation. CDP provides scores for companies and cities based on their level of disclosure and their environmental leadership. We only reviewed the Climate reports that were submitted for 2020, which means data are from 2019. We recorded the scores each company received and from each report pulled out specific pieces of information about each company, including active climate goals from 2019 (both absolute and intensity goals), baseline emissions data for those goals, and emissions for all three scopes from 2019. When SBTi and CDP data were not available, we used company corporate sustainability reports (CSRs). When no information was publicly available about company GHG emissions or goals, we were unable to evaluate them further.

2.3 Understanding Emissions and Targets

Emissions can be categorized as scope 1, scope 2, and scope 3 (Figure 1A). Scope 1 emissions are those that a company is directly responsible for, such as those released from their owned and operated plants and factories. Scope 2 emissions are indirectly produced by the company, such as the emissions generated by the purchased electricity, heating, and cooling required by the company's own plants and factories. These types of emissions are most easily accounted for and managed. Scope 3 emissions are all other emissions, most often associated

with the company’s value chain, such as the upstream emissions from growing crops for the product and downstream emissions produced when customers use the product. For food and beverage companies with upstream value chains in agriculture, scope 3 emissions make up the majority of their total emissions (Tidy et al. 2016) (Figure 1B). However, companies have historically had less visibility and influence over the operations producing their scope 3 emissions, so measuring and managing them can be challenging. Here, we evaluate the top 100 global food and beverage companies’ GHG reporting practices for these three scopes.

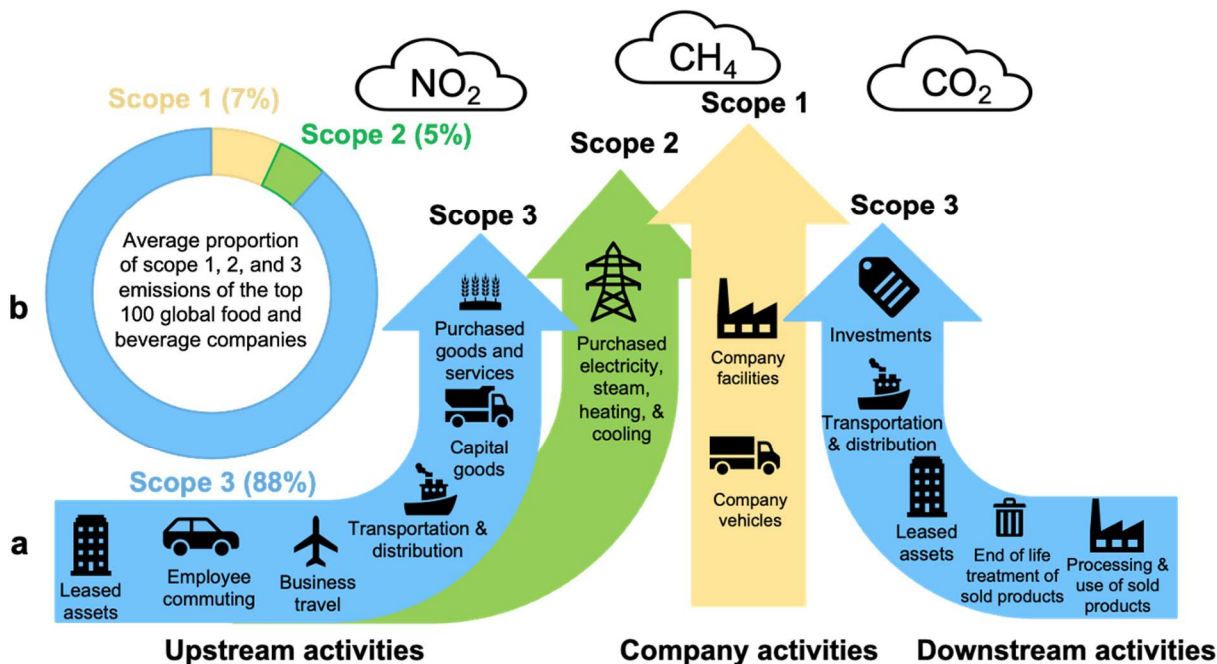


Figure 1. Distribution of scope 1, 2, and 3 emissions. The breakdown of total emissions into scope 1, 2 and 3 emissions of the top 100 global food and beverage companies (a) and the average proportion of scope 1, 2 and 3 greenhouse gas emissions (b).

For this research, we compared company goals to two standards that are aligned with what science says is necessary to keep global temperatures from warming more than 2 °C: the 3% Solution and the SBTi. The 3% Solution is a report, produced by WWF and CDP in 2013, that calculated how U.S. businesses could reach 25% of the IPCC’s 2 °C goal by reducing GHG

emissions 3% each year between 2010 and 2020 (Tcholak-Antitch et al. 2013). After reaching that target in 2020, a 4.3% annual reduction in emissions would be required each year until 2050 to meet 100% of that goal. To align with this standard, companies must set targets that reduce emissions at least 4.3% each year over the life of the target. The SBTi has two emission scenarios by which companies can set targets: well below 2 °C where emissions must decrease at least 2.5% each year, and 1.5 °C where emissions must decrease at least 4.2% per year (setting a target aligned with the 2 °C emission scenario, which called for at least 1.23% annual decrease, is no longer allowed for scope 1 and 2 emissions, but *is* allowed for scope 3 emission targets) (SBTi 2021b). While the 3% Solution requires a reduction of all emissions produced by the company, the SBTi standards focus on scope 1 and 2 emissions. Companies following the well below 2 °C scenario are also setting targets far less stringent than those of the 1.5 °C scenario or the 3% Solution standards. To evaluate company targets, we calculated the linear emission reductions over the lifespan of the target for total reported emissions and for reported scope 1 and 2 emissions only and compared them to the 3% Solution and SBTi emission scenarios.

2.4 Target Evaluation

We collected data on climate goals and scope 1, 2, and 3 emissions from the SBTi targets, CDP climate reports, and annual corporate responsibility reports for each company. We used the latest available data (2019 data from 2020 reports) from each company to identify presence, type, and extent of its climate goals. Companies could have two types of targets: absolute and intensity. Absolute targets aim to reduce overall emissions over a period of time (e.g., reduce absolute scope 1 and 2 emissions 20% by 2030 from a 2015 baseline). Intensity targets reduce the emissions required to produce some unit of measurement (e.g., reduce scope 3

GHG emissions 20% per ton of product by 2030 from a 2015 baseline). Some companies may be hesitant to set absolute goals, seeing them as potentially limiting future business growth, gravitating instead towards only intensity goals. However, both absolute and intensity targets are useful in different ways (SBTi 2021b). Absolute goals are often ambitious and aim to reduce the total GHGs entering the atmosphere. Intensity goals can reflect efficiency improvements and allow for comparison among peers. Having and meeting both types of goals ensure that overall emissions go down and production efficiency goes up. Some companies had climate targets that ended in 2020, we only include 2020 targets when any other (intensity or absolute) future target is not available. For example, when evaluating a company with an absolute target with a 2030 end date and an intensity target with a 2020 end date, we only evaluate the company on its 2030 goal, not 2020 goal.

We compared a company's baseline emission data to its current emissions to understand whether the company is on track towards reaching the proposed goals or, at the minimum, has reduced its current emissions compared to the baseline. (In CDP reports, companies are asked to disclose both market- and location-based scope 2 emissions. If the company specifies which scope 2 emissions they are tracking for their emissions targets, we used the specified scope 2 emissions for calculations. For companies that did not specify market or location, we used location-based scope 2 emissions. When calculating average scope 1, 2, and 3 emissions across all companies, we did not include companies that did not have full emission disclosure across all 3 scopes.) Over time, companies more accurately calculate and measure their emissions, which changes the scope of the emissions included under the baseline emissions. This makes comparing current total emissions to the baseline difficult if the company has measured additional aspects of their total emissions. Actual current emissions data was often much greater than the current

emissions reported if not all emission categories were included in the goal or if new areas of emission have since emerged and been measured that were not part of the original goal's range. For this research, we compared only the emission categories included in both the baseline and current emissions, since that is how the companies are measuring their progress on the goal. We note that this standard is imperfect and may not portray an entirely true picture of the state of things. Companies need to be clear about what targets they are claiming to meet and what portion of their total emissions they are addressing and reducing.

As mentioned previously, we compared company goals to the metrics of the 3% Solution, but this is only possible for companies with absolute targets. We could not evaluate intensity targets because production numbers to go along with the intensity are not provided with emission data, another limitation of the data. Only 17 companies had absolute targets and baseline data for all scopes, while 27 others had absolute targets and baseline data for scope 1 and 2 only.

3. RESULTS AND DISCUSSION

3.1 Extent of Publicly Disclosed GHG Emissions and Climate Goals

3.1.1 Emissions Disclosure

Of the 100 companies evaluated, 71 disclosed current scope 1 and 2 emissions data while 29 did not publicly disclose any of their emissions (Figure 2). Sixty-one companies disclosed at least partial scope 3 emissions, where they had measured some aspects of their value chain but had not mapped it entirely. Only 51 out of 100 companies measured and reported their scope 3 emissions across their entire value chain. While only half of the large food and beverage companies have disclosed their total emissions, this number also indicates a growing trend towards transparency in GHG emissions disclosure. A 2018 study of the top 50 food and

beverage companies found that only 32% (17) of companies were disclosing their emissions fully across all three scopes (Ceres 2019). This number more than doubled in our 2020 report data to 72% (36 of the top 50 companies). The fact that, in just two years, we see a 112% increase in the number of top 50 food and beverage companies reporting their entire scope 1, 2, and 3 emissions demonstrates a growing awareness and change in the industry.

Companies disclosed their GHG emissions primarily through CDP reports. Sixty-seven companies submitted Climate reports to CDP in 2020, and only 61 companies had publicly accessible Climate reports (Figure 2). The six other unavailable reports were submitted to CDP but not accessible because the companies had chosen not to disclose their report publicly (CDP staff, personal communication, April 14, 2021). Six companies with submitted reports were not scored by CDP for unknown reasons. CDP scores companies as a way to measure their “progress towards environmental stewardship” (CDP 2020). Companies earn points for their level of detail on disclosed information related to company climate policy, targets, and emissions and their display of understanding of climate change issues and progress made and planned towards climate change action. A summary of the breakdown of CDP scores can be found in Table 1.

ASA	CCJ	MAR	MCB	NES	PEP	SUN	ANA	HOR	SDL
BRY	DIA	KEL	MCC	NFG	AHB	AJI	FLF	JBS	OSI
CCC	GNM	KRH	MON	SCH	PER	SAP	HER	JRS	PER
CCE	KDP	DAN	CAR	UNI	ITO	CON	CAB	LAC	CMD
CCF	AJI	CLB	BAR	MAF	TTP	LND	FER	MFL	DMK
ABF	SMF	HBC	JMS	ING	BRF	BAC	DAC	DFC	SUD
TYS	FON	HEI	KHC	MEI	ARL	KER	OET	ITY	THB
BUN	GRB	NSG	LVMH	RFC	DFA	PHS	HWG	LBW	TSB
CAM	SAH	MOR	THF	VIO	EJG	SAV	AGR	LOL	YAM
ADM	NHF	MNC	NSU	MLG	RDB	JDE	CHS	MBG	YIG

Dark Green	Has CDP report, has scope 1, 2, and 3 absolute goals, has scope 1, 2, and 3 disclosure
Medium Green	Has CDP report, has scope 1, 2, and 3 goals, has scope 1, 2, and 3 disclosure
Light Green	Has CDP report, has scope 1, 2, and 3 goals, has scope 1 and 2 disclosure
Very Light Green	Has CDP report, has scope 1 and 2 goals, has scope 1, 2, and 3 disclosure
Lightest Green	Has CDP report, has scope 1 and 2 goals, has scope 1 and 2 disclosure
White	Has CDP report, lacks climate goals, has scope 1, 2, and 3 disclosure
Light Gray	Has CDP report, lacks climate goals, has scope 1 and 2 disclosure
Medium Gray	Lacks CDP report, has scope 1, 2, and 3 goals, has scope 1, 2, and 3 disclosure
Dark Gray	Lacks CDP report, has scope 1, 2, and 3 goals, has scope 1 and 2 disclosure
Very Dark Gray	Lacks CDP report, has scope 1, 2 and 3 goals, lacks emission disclosure
Black	Lacks CDP report, has scope 1 and 2 climate goals, lacks emission disclosure
Dark Black	Lacks CDP report, lacks climate goals, has some scope 1 and 2 disclosure
Blackest	Lacks CDP report, lacks climate goals, lacks emission disclosure

Figure 2. Heat map of company emission and goal disclosure.

Heat map showing the distribution of where all 100 companies have set goals and disclosed their emissions as of January 2021. Each box contains an abbreviation for one company. Company abbreviations can be found in Supplementary Information Table S1.

Table 1 Breakdown of CDP scores of those 61 companies with available scores.

Score	% of Companies	Number of Companies
A or A-	41	25
B or B-	41	25
C	15	9
D	3	2

Note: 61 companies had available CDPs, and 61 had available scores, but these are not necessarily the same 61 companies. Some companies with available reports were not scored, and some companies with scores did not have available reports.

Companies that participate in CDP reporting do so for various reasons including corporate stewardship or pressure from customers, retailers, and/or investors. Of the companies without submitted CDP reports, 16 were either not asked by investors or customers to participate in CDP reporting or did not volunteer to do so themselves (CDP staff, personal communication, April 4, 2021). Seventeen others were asked to submit reports by stakeholders, but they either declined or did not respond to the request. Eleven companies without CDP reports instead listed climate goals on their websites or corporate sustainability reports, and four of those companies' goals were approved by the SBTi. Only two companies disclosed all emission scopes without a CDP report (Figure 2). A CDP report is therefore not a required part of disclosing emissions or setting climate goals, but few large companies appear to do so otherwise.

3.1.2 Climate Goals

We found that 68 companies had some sort of climate goal in one or more scopes that extended beyond a 2020 end date (Figure 3). Forty of these had scope 1 and 2 absolute targets, 18 had scope 1 intensity targets, 17 had scope 2 intensity targets, and 10 had both absolute and intensity targets for scopes 1 and 2. Forty-one companies had targets that included all three emission scopes. (As noted previously, 51 companies fully disclosed emissions for all three scopes. However, not all companies with scope 3 goals disclosed all of their scope 3 emissions, and some companies that did fully disclose their emissions did not have scope 3 goals.) Twenty-two of the 37 science-based goals (which all include scope 3 emissions) were set by companies in 2019 or later. The rise in scope 3 targets, as with the rise in scope 3 emission disclosure, is a harbinger of an acceleration in the rate of companies taking aggressive climate action.

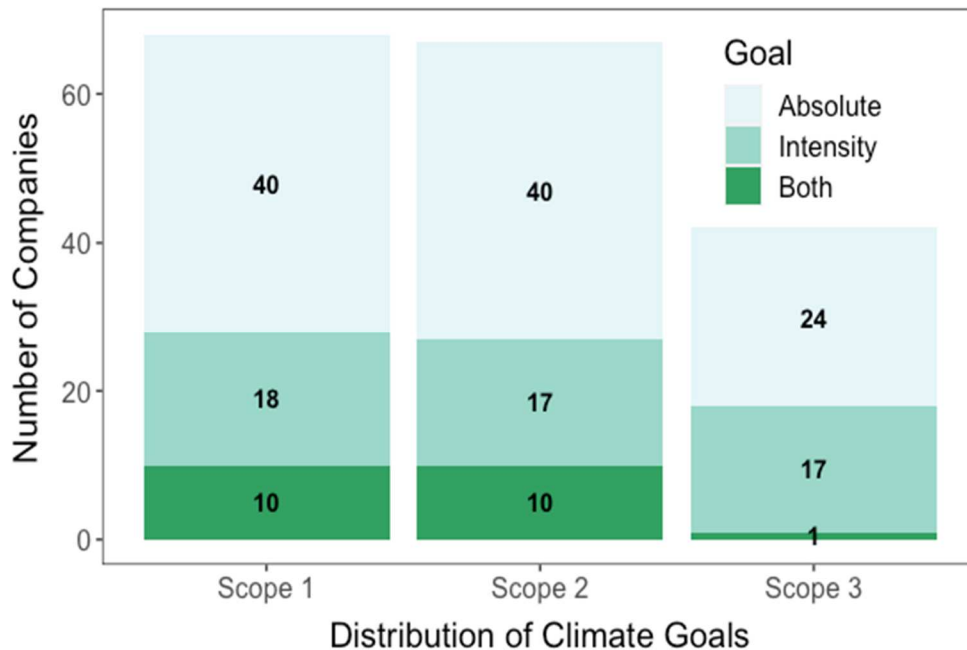


Figure 3. Distribution of absolute and intensity climate goals across scopes.

Number of food and beverage companies out of 100 that set absolute or intensity climate targets or both for scopes 1, 2, and 3. Numbers in the bars are how many companies fall into each category. Data show the number of goals active in 2019, reported in 2020 reports.

3.2 Areas for Improvement in Publicly Disclosed GHG Emissions and Climate Goals

After reviewing the publicly available climate data of these companies, we identified three areas with room for improvement in the way companies are currently disclosing their emissions and setting and monitoring climate goals: (1) the shortcomings in disclosure, (2) the difficulty in tracking progress towards goals, and (3) the lack of science-aligned goals.

3.2.1 Shortcomings in disclosure

As noted previously, we found that 49 companies are not disclosing their scope 3 emissions. Lack of disclosure from almost half of the largest food and beverage companies in the world shows the grim state of current monitoring and reporting practices in this industry, particularly since scope 3 emissions often make up the majority of a company's GHG emissions. Our analysis of the reported GHG emissions shows that scope 3 emissions contribute over 87% of the total emissions on average and can be as high as 99% (e.g., Nisshin Seifun Group, Constellation Brands, and Saputo). Scope 1 emissions made up an average of 7% and scope 2 emissions were about 5% of a company's total emissions. We believe an increase in scope 3 measurement and disclosure is necessary to understand the climate impact of this industry and to be able to effectively reduce overall emissions.

3.2.2 Difficulty in tracking progress toward goals

Three things were necessary in order to calculate whether or not a company is making progress towards its target: base year emissions, current (2019 in this study) emissions, and absolute targets for all scopes. Seventeen companies out of 100 had available data to match these criteria (Figure 4). Fifteen of these 17 companies have lower current emissions than their base

emissions, according to their reported emissions (companies noted in bold on the x-axis of Figure 4). The two other companies (companies not bolded on the x-axis of Figure 4) have increased their emissions from their baseline, making no progress on their targets. No mention of increasing their emissions was made in the reports of those two companies.

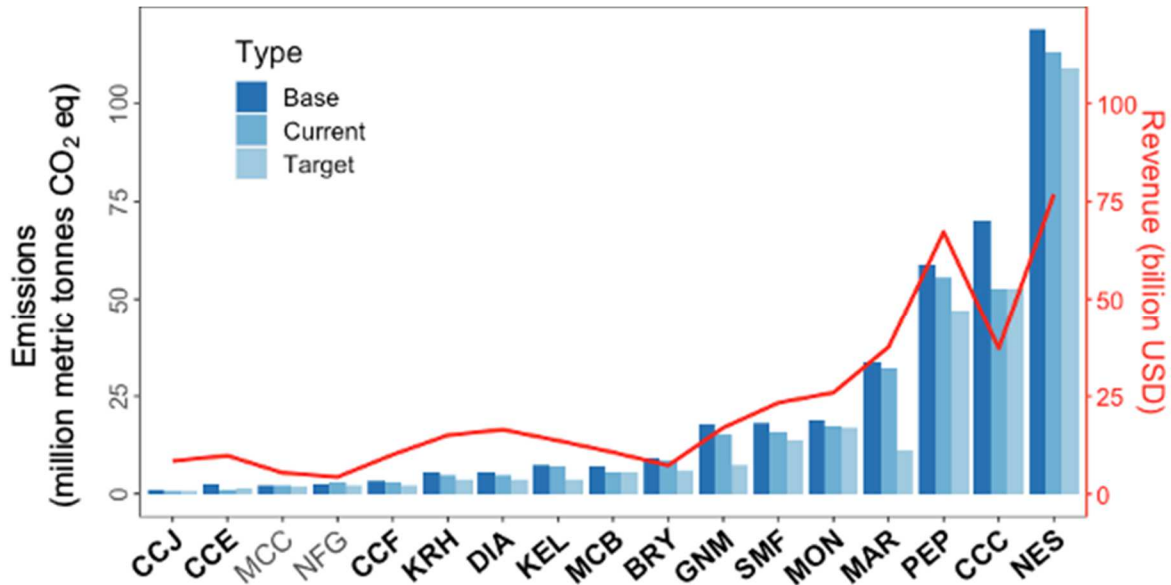


Figure 4 Base, current, and target year scope 1, 2, and 3 emissions for 17 companies. Distribution of base year emissions, current (2020 report) emissions, and target year emissions for seventeen companies with absolute targets and emissions data for scopes 1, 2, and 3. Red line and y-axis correspond to 2020 food sales revenue for each company in billions of USD. Acronyms left to right with base and target dates: Coca-Cola Bottlers Japan (CCJ: 2015-2030), Coca-Cola European Partners (CCE:2019-2030), McCormick Corporation (MCC; 2015-2025), Nissin Foods Group (NFG: 2018-2060), Coca-Cola Femsa (CCF: 2015-2030), Kirin Holdings (KRH: 2015-2030), Diageo (DIA: 2007-2020), Kellogg Company (KEL: 2015-2050), Molson Coors Brewing Co. (MCB: 2016-2025), Barry Callebaut (BRY: 2018-2025), General Mills (GNM: 2010-2050), Smithfield (SMF: 2010-2025), Mondelez International (MON), Mars (MAR: 2015-2025), PepsiCo (PEP: 2015-2030), The Coca-Cola Company (CCC: 2015-2030), Nestle (NES: 2014-2020). Company names in bold have reduced their emissions compared to baseline. Emissions data are acquired from 2020 CDP Climate reports submitted by each company, and revenue data are taken from Food Engineering’s 2020 list of top 100 food and beverage companies.

Such promising progress towards meeting climate goals may shroud the true state of things, though. As mentioned previously, actual company emissions are often greater than those reported towards their targets, since actual company emissions may include emission categories that are not included in the original target. In this set of 17 companies, eight companies had increased their emissions compared with their baselines when looking at their actual current emissions rather than reported ones, though in fact only two companies reported an increase. Since only 17 companies had absolute targets and baseline and current emission data for all three scopes, we expanded our criteria to include those without scope 3 targets or emission data.

There are 27 companies with scope 1 and 2 data and absolute scope 1 and 2 targets (Figure 5). Of these, 19 companies have reduced their emissions from their baselines (companies noted in bold on the x-axis of Figure 5) while eight companies have increased their emissions (non-bolded companies on the x-axis of Figure 5). As with the companies in Figure 4, reported emissions are often smaller than their actual emissions, meaning that while a company may be appearing to move towards their targets, actual emissions from the company are increasing. The discrepancies between actual and reported emissions make it difficult to accurately track reductions in overall company emissions. Tracking progress is made additionally arduous by the inability to always fully capture a company's goal and progress.

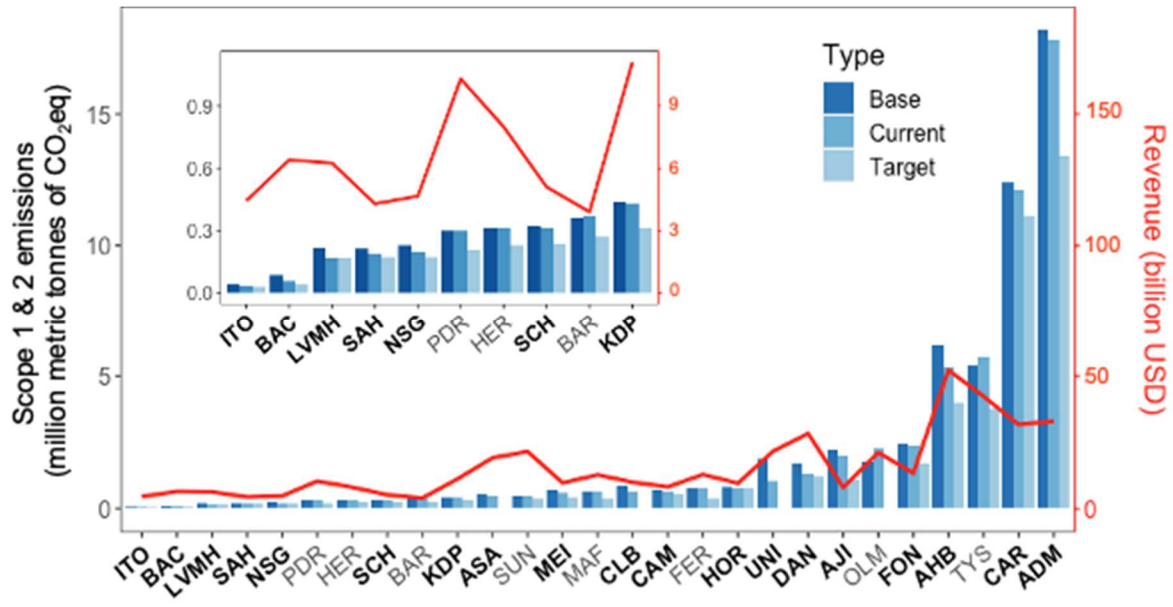


Figure 5. Base, current, and target year scope 1 and 2 emissions for 27 companies.

Distribution of base year emissions, current (2020 report) emissions, and target year emissions for twenty-seven companies with absolute targets and emissions data for scopes 1 and 2. Red line and y-axis correspond to 2020 revenue for each company in billions of USD. Smaller graph within is zoomed in on the smallest 10 companies. Acronyms left to right with base and target years: Ito En (ITO: 2018-2030), Bacardi (BAC: 2015-2025), LVMH (2013:2020), Sapporo Holdings (SAH: 2013-2030), Nisshin Seifun Group (NSG: 2013-2030), Pernod Ricard (PDR: 2018-2025), The Hershey Company (HER: 2015-2025), Schreiber Foods (SCH: 2017-2030), Barilla (BAR: 2017-2030), Keurig Dr. Pepper (KDP: 2018-2030), Asahi (ASA: 2015-2030), Suntory (SUN: 2015-2030), Meiji Holdings (MEI: 2015-2030), Marfrig Group (MAF: 2019-2035), Carlsberg Group (CLB: 2015-2030), Campbell Soup Company (CAM: 2017-2025), Ferrero (FER: 2018-2030), Hormel Foods Corporation (HOR: 2011-2020), Unilever (UNI: 2015-2030), Danone (DAN: 2015-2030), Ajinomoto (AJI: 2018-2030), Olam (OLM: 2017-2030), Fonterra (FON: 2018-2030), Anheuser-Busch (AHB: 2017-2025), Tyson (TYS: 2016-2030), Cargill (CAR: 2017-2025), Archer Daniel Midland (ADM: 2019-2035). Company names in bold have reduced their emissions from their baseline. Emissions data are acquired from 2020 CDP Climate reports submitted by each company, and revenue data are taken from Food Engineering’s 2020 list of top 100 food and beverage companies.

As mentioned previously, we can only evaluate companies’ *absolute* targets, as intensity targets are currently difficult to track because they require knowing the amount of product used in the metric, which is not often publicly available. Regardless of the metric of the target, the amount of units produced is required to measure progress toward the goal. In the CDP reports,

baseline, current, and target intensity numbers are provided, so it is possible to see whether progress is occurring, and estimated absolute reduction from the intensity targets is reported. However, we discovered a substantial number of errors and unverifiable numbers in the reports leading to questions about the reported numbers. Currently, CDP reports do not ask companies to submit data about production, so we cannot verify whether intensity goals are being met, but this may be a helpful aspect to include moving forward so that progress to reduce total emissions is accurately monitored.

Many of these companies with absolute scope 1 and 2 targets also have intensity targets covering these scopes or have additional scope 3 intensity targets. Three of the companies with increased emissions (SUN, MAF, OLM; Figure 5) also claimed increased business growth in the CDP reports. As businesses grow, emissions often grow as well, making absolute targets more difficult to meet. All three of these companies, though, had met or were making progress towards meeting their intensity targets. Strong intensity targets can contribute to overall absolute emission reductions (SBTi 2021b), so being unable to account for a company's progress on its intensity goals is a significant shortcoming to tracking company progress towards overall emission reduction.

3.2.3 Lack of science-aligned goals

In addition to examining how companies are progressing on their goals, we also evaluated their goals in comparison with a 3% Solution target estimation. Both The 3% Solution and the SBTi have standards for this annual emission reduction and multiple scenarios for reduction. We compared the company goals to five different scenarios: are they in line with a) a 4.3% annual reduction of total company emissions, b) a 3% annual reduction of total company

emissions, c) a 4.2% annual reduction of scope 1 and 2 emissions, d) a 2.5% annual reduction of scope 1 and 2 emissions, and e) a 1.23% annual reduction of scope 1 and 2 emissions? Scenarios a) and b) are based on the 3% Solutions, where prior to 2020, annual reduction needed to be at least 3%, but after 2020, reduction must be at least 4.3%. Scenarios c), d), and e) follow the SBTi guidelines, which only include rules for scopes 1 and 2.

Only the 17 companies included in Figure 4 were evaluated on the 3% Solution scenarios since the rest did not have full baseline scopes to compare with. Of those 17, four companies (CCE, BRY, GNM, MAR) have targets that are equally or more than aligned with the 3% Solution. We included all companies from Figures 4 and 5 when comparing with SBTi guidelines. Under the 4.2% annual scope 1 and 2 reduction scenario, 13 companies out of 44 are aligned. Twenty-six companies have targets aligned with a 2.5% annual scope 1 and 2 reduction scenario, and 37 are aligned with a 1.23% annual scope 1 and 2 reduction. Thirty-three of these companies have official science-based targets approved by the SBTi, meaning they must be aligned with at least one of these scenarios, though the 1.23% reduction scenario is no longer allowed. We found that two companies (MON, CAR) did not have targets that align with the SBTi guidelines, though it could have been that we were not able to make accurate calculations. MON target included all three emission scopes and did not provide separate scope 1 and 2 baseline emissions, so we were not able to accurately measure. CAR had an intensity goal as well which we are not able to measure.

For companies with large scope 3 emissions, it is hard to imagine that targets are truly science-based if they do not include scope 3. The IPCC estimates that global emissions must fall by at least 45% by 2030 from a 2010 baseline in order to limit warming to 1.5 °C (IPCC 2018). Scope 1 and 2 emissions from food and beverage companies often make up less than 45% of

their total emissions, so even targets that aim for zero emissions from scopes 1 and 2 fall short of this global goal if they do not include scope 3. Due to the difficulty of controlling some aspects of scope 3 emissions, including suppliers and other actors in the value chain in measuring and reducing their emissions will be critical in reaching global climate goals (NewClimate Institute and Data-Driven EnvironLab 2020). Transparent communication around scope 3 emissions and targets is important for facilitating constructive dialogue around challenges and moving towards closing the gaps in action (NewClimate Institute and Data-Driven EnvironLab 2020).

4. CONCLUSIONS

Our results present the current disclosure and emission goals of the largest food and beverage companies and highlight an urgent need to begin and continue to set truly ambitious, science-aligned climate goals. On the whole, the number of companies setting goals and disclosing emissions is increasing, but we found that 31 of the largest companies in this sector still do not have any climate goals. Of the ones that do have goals, half are not measuring, reporting on, or including scope 3 emissions. Since scope 3 emissions make up about 87% of these companies' total emissions on average, not monitoring or setting targets to reduce these emissions does little to reach the goal of keeping global warming to well below 2 °C. Reaching this goal is only possible if companies are setting climate targets that support and are aligned with the goal. As a first step towards achieving this goal, the global food and beverage sector needs to publicly disclose scope 1, 2 and 3 emissions for transparency and verification, monitor and report absolute and intensity targets, and set climate goals aligned with science-based targets.

ACKNOWLEDGMENTS

The NSF Intern Award (supplement to MCB-1716844) funded this study. We are thankful for the Environmental Defense Fund, Bentonville, AR for hosting MR as an Intern.

AUTHOR CONTRIBUTION

MR designed this study and analyzed the data with assistance of JA, JR, and KN. MR wrote the initial manuscript draft with contributions from KN, JA, and JR. All authors discussed, edited, revised, and approved the paper.

DECLARATION OF CONFLICT

Authors declare no conflict of interests.

DATA AVAILABILITY

All data used in this study were obtained from publicly available sources, which are noted for each company in Supplementary Table S1.

AUTHOR LIST

Megan Reavis^{1*}, Jenny Ahlen², Joe Rudek², and Kusum Naithani¹

¹ *University of Arkansas, Department of Biological Sciences, Fayetteville, AR, United States*

² *Environmental Defense Fund, New York, NY, United States*

**ml008@uark.edu*

5. REFERENCES

CDP (2020). CDP Homepage. Available at: <https://www.cdp.net/en> [Accessed February 22, 2021].

Ceres (2019). Top US Food and Beverage Companies Scope 3 Emissions Disclosure and Reductions. Engage the Chain. Available at: <https://engagethechain.org/top-us-food-and-beverage464-companies-scope-3-emissions-disclosure-and-reductions> [Accessed February 12, 2021].

- Christensen, J., and Olhoff, A. (2019). Lessons from a decade of emissions gap assessments. Nairobi: United Nations Environment Programme Available at: <https://wedocs.unep.org/bitstream/handle/20.500.11822/30022/EGR10.pdf?sequence=1&isAllow468ed=y> [Accessed February 12, 2021]. 469
- Crippa, M., Solazzo, E., Guizzardi, D., Monforti-Ferrario, F., Tubiello, F. N., and Leip, A. (2021). Food systems are responsible for a third of global anthropogenic GHG emissions. *Nat Food* 2, 198– 471 209. doi:10.1038/s43016-021-00225-9.
- Faria, P. (2016). The evolution of corporate climate targets. We Mean Business Coalition. Available at: <https://www.wemeanbusinesscoalition.org/blog/the-evolution-of-corporate-climate-targets/> [Accessed February 12, 2021].
- Food Engineering (2020). 2020 Top 100 Food & Beverage Companies | Food Engineering. Available at: <https://www.foodengineeringmag.com/2020-top-100-food-beverage-companies> [Accessed 477 February 12, 2021].
- Gerber, P. J., Steinfeld, H., Henderson, B., Mottet, A., Opio, C., Djikman, J., et al. (2013). Tackling climate change through livestock - a global assessment of emissions and mitigation opportunities. Rome: Food and Agriculture Organization of the United Nations.
- GRAIN (2018). Emissions impossible: How big meat and dairy are heating up the planet. Available at: <https://grain.org/article/entries/5976-emissions-impossible-how-big-meat-and-dairy-are-heating-up-the-planet> [Accessed April 21, 2021].
- Haffar, M., and Searcy, C. (2018). Target-setting for ecological resilience: Are companies setting environmental sustainability targets in line with planetary thresholds? *Business Strategy and the Environment* 27, 1079–1092. doi:10.1002/bse.2053.
- IPCC (2021). Climate Change 2021: The Physical Science Basis. Contribution of Working Group I to the Sixth Assessment Report of the Intergovernmental Panel on Climate Change [Masson-Delmotte, V., P. Zhai, A. Pirani, S.L. Connors, C. Péan, S. Berger, N. Caud, Y. Chen, L. Goldfarb, M.I. Gomis, M. Huang, K. Leitzell, E. Lonnoy, J.B.R. Matthews, T.K. Maycock, T. Waterfield, O. Yelekçi, R. Yu, and B. Zhou (eds.)]. Cambridge University Press. In Press. Available at: <https://www.ipcc.ch/report/ar6/wg1/#FullReport> [Accessed October 4, 2021].
- Kobayashi, N., and Richards, M. (2021). Global Sector Strategies: Recommended Investor Expectations for Food and Beverage. Ceres Available at: <https://www.climateaction100.org/wpcontent/uploads/2021/08/Global-Sector-Strategies-Food-and-Beverage-Ceres-PRI-August2021.pdf> [Accessed September 14, 2021].
- Lai, A., and Schiano, S. (2021). Empowered Consumers Go Green. Forrester. Available at: <https://www.forrester.com/report/Empowered+Consumers+Go+Green/-/RES163526?objectid=RES163526> [Accessed February 12, 2021].NewClimate

- Institute, and Data-Driven EnvironLab (2020). Navigating the nuances of net-zero targets. Available at: https://newclimate.org/wpcontent/uploads/2020/10/NewClimate_NetZeroReport_October2020.pdf [Accessed June 4, 2021]. Plunkett Research, Ltd. (2021).
- Plunkett's Food Industry Market Research. Food, Beverage and Grocery Overview. Available at: <https://www.plunkettresearch.com/industries/food-beverage-grocery506-market-research/> [Accessed May 10, 2021].
- Reid, P. C., Hari, R. E., Beaugrand, G., Livingstone, D. M., Marty, C., Straile, D., et al. (2016). Global 508 impacts of the 1980s regime shift. *Global Change Biology* 22, 682–703. doi:<https://doi.org/10.1111/gcb.13106>.
- Rijsberman, F. R., and Swart, R. J. (1990). Targets and indicators of climatic change. Stockholm: Stockholm Environment Institute.
- Ripple, W. J., Wolf, C., Newsome, T. M., Barnard, P., and Moomaw, W. R. (2019). World Scientists' Warning of a Climate Emergency. *BioScience* 70, 8–12. doi:[10.1093/biosci/biz088](https://doi.org/10.1093/biosci/biz088).
- Ritchie, H. (2019). Food production is responsible for one-quarter of the world's greenhouse gas emissions. Our World in Data. Available at: <https://ourworldindata.org/food-ghg-emissions> [Accessed February 12, 2021].
- Sax, S. (2020). Employees Are Fighting for a New Cause at Work: The Climate. EcoWatch. Available at: <https://www.ecowatch.com/employee-climate-activism-2645855023.html> [Accessed February 12, 2021].
- SBTi (2021a). Companies taking action. Science Based Targets. Available at: <https://sciencebasedtargets.org/companies-taking-action> [Accessed February 12, 2021].
- SBTi (2021b). SBTi Corporate Manual. SBTi Available at: [file:///Users/meganreavis/Downloads/SBTi Corporate-Manual-v1.0-2.pdf](file:///Users/meganreavis/Downloads/SBTi%20Corporate-Manual-v1.0-2.pdf) [Accessed February 12, 2021].
- Searchinger, T., Waite, R., Hanson, C., and Ranganathan, J. (2019). Creating a Sustainable Food Future: A Menu of Solutions to Feed Nearly 10 Billion People by 2050. World Resources Institute Available at: https://research.wri.org/sites/default/files/2019-07/WRR_Food_Full_Report_0.pdf [Accessed February 12, 2021].
- Tcholak-Antitch, Z., Carnac, T., Harris, C., Baker, B., Banks, M., Gerholdt, R., et al. (2013). The 3% Solution: Driving Profits Through Carbon Reduction. Available at: https://c402277.ssl.cf1.rackcdn.com/publications/575/files/original/The_3_Percent_Solution_June_10.pdf?1371151781 [Accessed February 12, 2021].

Tidy, M., Wang, X., and Hall, M. (2016). The role of Supplier Relationship Management in reducing Greenhouse Gas emissions from food supply chains: supplier engagement in the UK supermarket sector. *Journal of Cleaner Production* 112, 3294–3305. doi:10.1016/j.jclepro.2015.10.065.

Winston, A. (2017). The Rise of Corporate Sustainability Goals: Some Hard Data. *Sustainable Brands*. Available at: <https://sustainablebrands.com/read/marketing-and-comms/the-rise-of-corporate-sustainability-goals-some-hard-data> [Accessed February 12, 2021].

SUPPLEMENTARY INFORMATION

Supplementary Table S1. Information on all companies used in this study.

Companies listed alphabetically that were used in this study, along with where data for each company was obtained, the company headquarters, and the ranking of each company on Food Engineering's top 100 list [#]. Data was primarily obtained from CDP reports (which can be found by searching the company on CDP's website: <https://www.cdp.net/en/scores>), the Science Based Targets Initiative (SBTi, which can be found on their website: <https://sciencebasedtargets.org/companies-taking-action>), or company websites (given in table).

Company	Abbreviation	Where data were obtained	Headquarters	Food Engineering Placement
Agropur Cooperative	AGR	https://www.savencia-fromagedairy.com/rapportanuel_EN_2019/pdf/savencia_RA.pdf	St. Hubert, Longueuil, Canada	81
Ajinomoto	AJI	CDP report	Tokyo, Japan	59
Anadolu Efes	ANA	CDP report	Istanbul, Turkey	96
Anheuser-Busch InBev	AHB	CDP report	St. Louis, MO, USA	3
Archer Daniels Midland Company	ADM	CDP report	Chicago IL, USA	8
Arla Foods	ARL	SBTi	Viby, Denmark	34
Asahi	ASA	CDP report	Tokyo, Japan	19
Associated British Foods	ABF	CDP report	London, UK	42
Bacardi	BAC	https://d3bbd6es2y3ctk.cloudfront.net/wp-content/uploads/2020/02/12184711/CR_Report_2019.pdf	Hamilton, Bermuda	71
Barilla	BAR	2 CDP reports (2020, 2018)	Parma, Italy	99
Barry Callebaut	BRY	CDP report	Zurich, Switzerland	65
Brf Brasil Foods	BRF	https://www.brf-global.com/wp-content/uploads/2020/05/BRF-RI-2019-EN.pdf	Santa Catarina, Brazil	50
Bunge	BUN	CDP report on website: https://www.bunge.com/sites/default/files/2020_global_sustainability_report.pdf	Chesterfield, MO, USA	33
Campbell Soup Company	CAM	CDP report	Camden, NJ, USA	56
Cargill	CAR	CDP report	Wayzata, MN, USA	9
Carlsberg Breweries	CLB	CDP report	Copenhagen, Denmark	44

Table 1 Continued				
Company	Abbreviation	Where data were obtained	Headquarters	Food Engineering Placement
China Mengniu Dairy Co.	CMD	http://iis.quamnet.com/media/IRAnnouncement/2319/EN_US/9353818-0.PDF	Causeway Bay, Hong Kong	35
CHS	CHS	https://www.chsinc.com/about-chs/sustainability#:~:text=At%20CHS%2C%20we%20are%20passionate,to%20learn%20and%20thrive%20together.	Inver Grove Heights, MN, USA	20
Coca Cola European Partners	CCE	CDP report	United Kingdom	27
Cocacola Bottlers Japan	CCJ	CDP report	Tokyo, Japan	52
Cocacola Femsa	CCF	CDP report	Mexico City, Mexico	43
Cocacola HBC	HBC	CDP report	Zug, Switzerland	60
ConAgra Brands	CAB	CDP report	Chicago IL, USA	46
Constellation Brands	CON	CDP report	Victor, NY, USA	53
Dairy Farmers of America	DFA	https://issuu.com/dairyfarmersofamerica/docs/sustbk1901_ssr_pages_fnl?fr=sOWNkNzEwNzA5MDM	Kansas City, KS, USA	23
Danish Crown	DAC	https://www.danishcrown.com/media/6892/2019-2020_sustainability-report.pdf?63741373305000000	Randers, Denmark	51
Danone	DAN	CDP report	Paris, France	10
Dean Foods Company	DFC	https://www.deanfoods.com/our-story/corporate-responsibility/environmental-sustainability/	Dallas, TX, USA	64
Diageo	DIA	CDP report	London, UK	22
DMK Deutsches Milchkontor	DMK	https://www.dmk.de/wer-wir-sind/geschaeftsbericht-2019/nachhaltigkeit-verantwortung/	Waren, Germany	67
E&J Gallo Winery	EJG	https://www.gallo.com/files/Corporate_Social_Responsibility_Brochure_2020.pdf	Modesto, CA, USA	85

Table 1 Continued				
Company	Abbreviation	Where data were obtained	Headquarters	Food Engineering Placement
Ferrero	FER	https://www.ferrerosustainability.com/int/sites/ferrerosustainability_int/files/2020-12/ferrero_sr19_final.pdf	Alba, Italy	30
Flowers Foods	FLF	CDP report	Thomasville, GA, USA	95
Fonterra	FON	CDP report	Auckland, New Zealand	28
General Mills	GNM	CDP report	Minneapolis, MN, USA	21
Grupo Bimbo (Mexico)	GRB	CDP report	Mexico City, Mexico	24
Hangzhou Wahaha Group	HWG	no information	Hanzhou, China	58
Heineken	HEI	CDP report	Amsterdam, Netherlands	11
Hormel Foods Corporation	HOR	CDP Report https://www.hormelfoods.com/responsibility/our-approach-to-issues-that-matter/environment/	Austin, MN, USA	47
Ingredion Inc.	ING	CDP report	Westchester, IL, USA	75
Inner Mongolia Yili Industrial Group	YIG	https://tinyurl.com/2hwa95vk	Hohhot, Inner Mongolia	29
Ito En	ITO	CDP report	Tokyo, Japan	89
Itoham Yonekyu	ITY	https://www.itoham-yonekyu-holdings.com/english/	Tokyo, Japan	61
J R Simplot	JRS	https://www.simplot.com/sustainability	Boise, ID, USA	94
Jacobs Douwe Egberts	JDE	https://www.jacobsdouweegberts.com/siteassets/sustainability/jde-cr-report-2019---v011---final---web.pdf	Amsterdam, Netherlands	70
JBS	JBS	CDP report	Greeley, CO, USA	4
Kellogg Company	KEL	CDP report	Battle Creek, MI, USA	26
Kerry Group	KER	SBTi	Tralee, Ireland	55
Keurig Dr Pepper	KDP	CDP report	Plano, TX, USA	37
Kirin Holdings	KRH	CDP report	Nakano City, Tokyo, Japan	25
Kraft-Heinz Company	KHC	CDP report	Chicago IL, USA	13

Table 1 Continued				
Company	Abbreviation	Where data were obtained	Headquarters	Food Engineering Placement
Lactalis	LAC	https://www.lactalisingredients.com/wp-content/uploads/2020/06/Lactalis-Ingredients-CSR-report-2019.pdf	Laval, France	18
Lamb Weston	LBW	CDP report	Eagle, ID, USA	100
Land O- Lakes Inc	LOL	CDP report	Arden Hills, MN, USA	98
Lindt & Sprungli	LDT	CDP report	Zurich, Switzerland	88
LVMH	LVMH	CDP report	Paris, France	74
Marfrig Group	MAF	CDP report	State of Sao Paulo, Brazil	31
Mars	MAR	CDP report	McLean, VA, USA	6
Maruha Nichiro Corp	MNC	https://www.maruhanichiro.com/sustainability/pdf/report2020_en.pdf	Tokyo, Japan	54
McCain Foods Ltd	MFL	https://www.mccain.com/media/3377/mccainfoods_sustainabilityreport2019.pdf	Toronto, Canada	41
McCormick Corporation	MCC	CDP report	Baltimore, MD, USA	82
Meiji Holdings	MEI	CDP report https://www.meiji.com/global/sustainability/esg/pdf/esg.pdf#page=3	Tokyo, Japan	45
Molson Coors Brewing Co.	MCB	CDP report	Chicago IL, USA	39
Mondelez International	MON	CDP report	Chicago IL, USA	12
Monster Beverage Corp	MBC	https://www.monsterbeverage.com/sr-environmental.php	Corona, CA, USA	93
Morinaga Milk Industry	MOR	CDP report	Tokyo, Japan	83
Muller Group	MLG	https://www.mueller-group.com/en/group/sustainability.html	Fischach, Germany	72
Nestle	NES	CDP report	Vevey, Switzerland	1
NH Foods	NHF	https://www.nipponham.co.jp/eng/csr/report/res/pdf/environmental_report.pdf	Osaka, Japan	38
Nisshin Seifun Group	NSG	CDP report	Tokyo, Japan	87
Nissin Foods Group	NFG	CDP report	Tokyo, Japan	90

Table 1 Continued				
Company	Abbreviation	Where data were obtained	Headquarters	Food Engineering Placement
Nissui	NIS	https://s3-ap-northeast-1.amazonaws.com/sustainability-cms-nissui-s3/pdf/en/2020_sustainability_digest_en.pdf	Tokyo, Japan	77
Oetker Group	OET	https://www.oetker-group.com/en/profile/sustainability	Bielefeld, Germany	66
Olam	OLM	CDP report	Singapore	17
OSI Group	OSI	https://www.osigroup.com/wp-content/uploads/OSI-2018-2019-Global-Sustainability-Report-web.pdf	Aurora, IL, USA	73
Pepsico	PEP	CDP report	Harrison, NY, USA	2
Perdue Farms	PER	https://corporate.perdufarm.com/company-stewardship-report-flipbook/index.html?page=22	Salisbury, MD, USA	86
Pernod Ricard	PDR	CDP report	Paris, France	40
Post Holdings	PTH	https://www.postholdings.com/wp-content/uploads/2020/12/PHI-2020-Environmental-Social-and-Governance-Report-12-3.pdf	St. Louis, MO, USA	78
Red Bull	RDB	https://www.redbull.com/int-en/energydrink/red-bull-can-lifecycle	Fuschl, Austria	69
Royal Friesland Campina	RFC	https://www.frieslandcampina.com/sustainability/	Amersfoort, Netherlands	32
Sapporo Holdings	SAH	CDP report	Tokyo, Japan	92
Saputo	SAP	CDP report on website (year 2020)	Montreal Canada	36
Savencia Fromage and Dairy	SAV	https://view.publitas.com/cfreport/vion-corporate-social-responsibility-report-2019/page/38	Viroflay, France	80
Schrieber Foods	SCH	CDP report	Green Bay, WI, USA	84
Smithfield Foods/WH Group	SMF	https://www.smithfieldfoods.com/pdf/sustainability/SMITHFIELD_CSR_Report.pdf	Smithfield, VA, USA	14
Sodiaal	SOD	https://translate.googleusercontent.com/translate_f	Paris, France	76

Table 1 Continued				
Company	Abbreviation	Where data were obtained	Headquarters	Food Engineering Placement
Sudzucker	SUD	https://www.suedzucker.de/en/company/sustainability/planet/energy-emissions	Mannheim, Germany	63
Suntory	SUN	CDP report	Tokyo, Japan	16
ThaiBev	THB	http://sustainability.thaibev.com/2019/en/climate_change.php	Bangkok, Thailand	49
The Coca-Cola Company	CCC	CDP report	Atlanta, GA, USA	7
The Hershey Company	HER	CDP report	Hershey, PA, USA	57
The JM Smuckers Company	JMS	CDP report	Orrville, OH, USA	62
Total Produce	TTP	https://www.totalproduce.com/content/uploads/2020/06/total-produce-sustainability-report-2020-web.pdf	Dundalk, Ireland	68
Treehouse Foods	THF	https://s23.q4cdn.com/884251494/files/doc_downloads/esg/2020/2020_esg_report/TreeHouse_2020_ESG_Report_Final_Reduced_Size.pdf	Oak Brook, IL, USA	91
Tsingtao Brewery	TSB	no information	Qingdao, China	97
Tyson	TYS	CDP report	Springdale, AR, USA	5
Unilever	UNI	CDP report	London, UK	15
Vion	VIO	https://view.publitas.com/cfrreport/vion-corporate-social-responsibility-report-2019/page/92	Boxtel, The Netherlands	79
Yamazaki Baking	YAM	https://www.yamazakipan.co.jp/english/e_initiatives/index.html	Tokyo, Japan	48

CHAPTER 2: Drought Response Curve: A Novel Mechanistic Method for Quantifying Phenotypic Expression of Drought Sensitivity in Crops

ABSTRACT

To ensure global food security, phenotyping crops for survival in future climates, including drought resistance, is urgently needed. Growing rice (*Oryza sativa*), a globally important cereal crop with high water requirement, in a drought prone future will need identification of genotypes that are resistant to drought. Popular modern methods of high throughput phenotyping screen a large number of plants for specific traits, but these methods lack the ability to directly measure photosynthesis, an important indicator of yield, and to predict plant response under stress. Here, we developed and tested a mechanistic model to predict the photosynthesis response to drought stress in eight rice genotypes (310588, 310723, 311620, 311677, 311795, 311792, Nagina 22, and Zhe 733). The model is a two-parameter Michaelis-Menten equation, with an A_{max} parameter, predicting maximum photosynthesis rate, and a PLA_{50} parameter, which describes the percent soil moisture at 50% loss of maximum assimilation. We tested the model on plants in manipulative field and growth chamber experiments, and validated model predictions of drought sensitivity with field generated yield data. Based on the PLA_{50} parameter values, we ranked these genotypes along a gradient of drought sensitivity. 311677 and 311795 were found to be most sensitive to drought, while 311792 and 311620 had a low sensitivity to drought. The parameter PLA_{50} provides a way to rank drought sensitivity of different genotypes and can be used to predict yield under stress in crop models.

1. INTRODUCTION

Rice is one of the largest food crops in the world and provides between 50-80% of the daily calories for many people in Asian countries (Mohanty et al., 2013). In 2018, nearly 500 million metric tons of milled rice were produced worldwide (Shahbandeh, 2019), however, highly water intensive, rice is expected to be one of the crops most affected by rising temperatures and droughts, which will occur with increasing frequency as the climate changes (Mohanty et al., 2013; Kissoudis et al., 2016). One of the grand challenges of the 21st century is to feed the growing human population without using more land while reducing greenhouse gas emissions and water use (Searchinger et al., 2019). We need novel methods to improve our understanding and capability to phenotype and predict crop response to changing climate.

Developing crops that can resist more frequent and intense droughts of future climates is one of the proposed solutions for future food security (Tuberosa, 2012; Kissoudis et al., 2016; Bailey-Serres et al., 2019; Searchinger et al., 2019). Past research reports have been focused on identifying genes for plant traits, including altered root architecture (Kitomi et al., 2020), cytokinin regulation (Hai et al., 2020), stomatal regulation (Caine et al., 2018), stay-green traits (Ba Hoang and Kobata, 2009), pathogen resistance (Zuluaga et al., 2020), and nutrient assimilation (Han et al., 2021), which may increase yields under drought (Tuberosa, 2012). Plant genomes are quite plastic and the interaction between genes and the environment can result in a great variety of phenotypes within a narrow range of genetic variation (Varshney et al., 2005). Understanding phenotypic plasticity requires linking the phenotypic performance of plants grown in both controlled and field environments (Sinclair et al., 2004; Fiorani and Schurr, 2013). Phenotypic screening for transferable traits under a gradient of environmental conditions is

necessary for predictive understanding of genotype response to external stressors and crop selection (Tuberosa, 2012; Araus and Cairns, 2014; Kissoudis et al., 2016; Costa et al., 2019).

High throughput phenotyping platforms are gaining popularity as they can screen hundreds to thousands of genotypes (Araus and Cairns, 2014; Ghanem et al., 2015). These platforms are image-based, use non-invasive technologies to measure variables like canopy and plant temperature (Babar et al., 2006; Deery et al., 2016), chlorophyll content (Babar et al., 2006; Sass et al., 2012), plant water status (Jones et al., 2009; Beverly et al., 2020) and leaf growth rates (Tackenberg, 2007; Tessmer et al., 2013), and are useful as an initial screening method to detect broad differences among genotypes (Ghanem et al., 2015). However, the rate of net photosynthesis is an important phenotypic trait that cannot be measured in a high throughput system. Several indirect methods have been developed to estimate photosynthesis in a high throughput platform, such as using chlorophyll fluorescence, thermal imagery, and normalized difference vegetation index (NDVI) (Furbank and Tester, 2011; Cruz et al., 2016; Silva-Perez et al., 2018). However, these methods are often difficult to transfer from controlled environments to field conditions (Tuberosa, 2012; Costa et al., 2019), and plant response under controlled conditions will likely differ from their response in field environments (Sultan, 2000). While modern high-throughput approaches are becoming increasingly common, there is growing need for quantification of phenotypic expression of plant traits under a gradient of environmental conditions and methods that are transferable from controlled experiments to field conditions for accurate plant selection and breeding (Varshney et al., 2005).

Photosynthesis response curves are commonly used to evaluate how the net rate of photosynthesis changes with changing environmental conditions, including light, CO₂, and temperature (Farquhar et al., 1980; Thornley and Johnson, 1990; Medlyn et al., 2002; Sharkey et

al., 2007). These response curves are useful in understanding the ecophysiology of plants, by estimating biochemical model parameters that can be used in crop models to predict photosynthetic response under a variety of environmental conditions (Herrmann et al., 2019). Previous studies have made significant progress in our understanding of how drought affects photosynthesis (Pinheiro and Chaves, 2011; Zargar et al., 2017; Wang et al., 2018; Yang et al., 2019), but we still lack quantitative models to phenotype drought sensitivity of plant genotypes under a gradient of soil moisture. With an overarching goal of quantifying the phenotypic expression of drought sensitivity in different rice genotypes, we asked the following 4 questions: (1) *Does photosynthesis follow a predictable pattern to progressive drought?* We selected three genotypes (310588, 310723, and 311795) on which to evaluate our model and test the hypothesis that photosynthesis response to progressive drought is quantifiable and predictable. We hypothesized that photosynthesis would increase with increasing soil water content with a saturating response in more sensitive genotypes, while there will be weak or no predictable pattern in less sensitive genotypes. (2) *Are these models transferable from a controlled environment to field conditions?* We subjected eight different genotypes to progressive drought in growth chambers and field plots to understand whether genotype model parameters differ between environments. (3) *Do model parameters from both environments correlate with yield?* Previous studies have highlighted the relationship between photosynthesis rates and crop yield (Amthor, 2007; Simkin et al., 2019; Wu et al., 2019). To test the hypothesis that models based on photosynthesis response to drought are useful in quantifying phenotypic expression of drought sensitivity of yield, we compared the model predictions of drought sensitivity with yield data collected under drought conditions.

2. MATERIALS AND METHOD

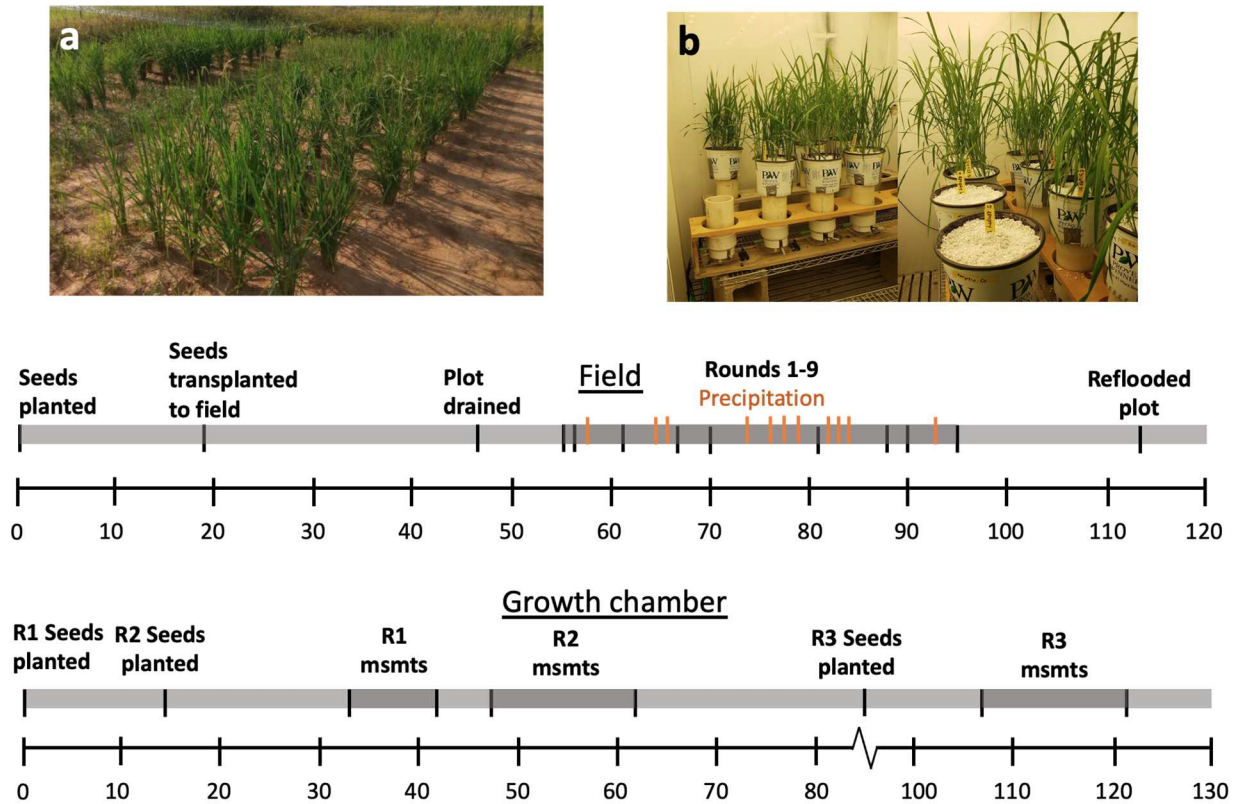


Figure 1. Experimental setup for (a) field and (b) growth chamber. The timelines display significant events throughout the two experiments in days after planting seeds. The growth chamber experiment was completed in 3 rounds, so R1, R2, and R3 refer to rounds 1, 2, and 3, respectively.

2.1 Plant Material

Seeds from six genotypes from the USDA rice mini-core collection and two additional genotypes were selected for this study: 310588, 310723, 311620, 311677, 311792, and 311795, and N22 and ZHE. N22 is known to have low sensitivity to drought (Kamoshita et al., 2008; Kumar, 2017; Poli et al., 2018), while 311795 has shown more sensitivity to drought (Kato et al., 2006; Degenkolbe et al., 2009; Kumar, 2017). The rest of the genotypes are not well studied, and we hope to further understand their relationship with drought by using a new method developed

in this study. The specific characteristics of each genotype as they are known are listed in Table 1.

Table 1. Description of selected rice genotype and their drought sensitivity.

Accession number	Genotype name	Taxon	Subgroup	Country of origin	Sensitivity to drought	Reference
310588	Onu B	<i>Oryza sativa</i>	TRJ	Zaire	unknown	---
310723	WIR 3039	<i>Oryza sativa</i>	AUS	Tajikistan	unknown	---
311620	Romeno	<i>Oryza sativa</i>	TEF	Portugal	unknown	---
311677	Karabaschak	<i>Oryza sativa</i>	TEJ	Bulgaria	unknown	---
311792	Cypress	<i>Oryza sativa</i>	TRJ	United States	unknown	---
311795	Nipponbare	<i>Oryza sativa</i>	TEJ	Japan	High sensitivity	Degenkolbe et al 2009, Henry et al 2011
---	Nagina 22	<i>Oryza sativa</i>	AUS	India	Low sensitivity	Kamoshito et al 2008, Poli et al 2013
---	Zhe733	<i>Oryza sativa</i>	IND	China	High sensitivity	Lafitte et al 2006

2.2 Growing Conditions

2.2.1 Pot Experiments

Plants were grown in a 5:1 potting soil and field soil (Pembroke silt loam (fine-silty, mixed, active, mesic Mollic Paleudalfs) and Pickwick wilt loam (fine-silty, mixed, semi-active, thermic Typic Paleudults), (USDA)) mixture in 3.8 L pots. Field soil had been dried and autoclaved to kill weed seeds. Many seeds were germinated in each pot but, after sprouting, were thinned to three plants per pot, with two pots for each genotype. All pots were kept well-watered

for 4 weeks in a greenhouse and then were transferred to a growth chamber. Lights in the growth chamber were set to $600 \mu\text{mol m}^{-2} \text{s}^{-1}$ on a 16:8 hour light:dark cycle. One pot per plant was randomly designated as the well-watered treatment and the other was assigned the drought treatment. Pots were labeled with a random number and placed in that random order on scales within the growth chamber. 60 g of perlite were added to each pot at the start of the experiment to prevent evaporation and ensure the only water loss from the pot was through transpiration from the leaves. Pots were weighed at field capacity and water was added each day to maintain that weight for the well-watered plants. Drought treatment pots were allowed to lose 80 g of water each day and water was added to pots after measurements if more was lost. Gas exchange and chlorophyll fluorescence were measured on each plant daily using an LI-6400XT-40 leaf chamber fluorometer (LI-COR Biosciences, Lincoln, NE, USA). Soil moisture was measured in each pot at the time of gas exchange measurements with a Dynamax SM150 Portable Soil Moisture Probe (Dynamax, Fresno, CA, USA). Drought was maintained for 14 days or until plant leaves were too rolled to measure or until photosynthesis was zero $\mu\text{mol m}^{-2} \text{s}^{-1}$. The whole experiment was repeated for three rounds.

2.2.2 Field Experiments

The same six genotypes, in addition to two more (311620 and 311792), were selected for the field experiment. Ten seeds of each genotype were germinated on 15 May 2019 in 0.95 L black pots with 1:1 mixture of potting soil and field soil. After 3 weeks, the plants were transplanted from the pots to the two 6.1 x 6.1 m levee-bound field plots at the University of Arkansas Division of Agriculture's Agriculture Experiment Station in Fayetteville, AR (36.096051° , -94.167418°). Plants were transplanted 0.3 m apart from each other in rows by

genotype. Fertilizer was scattered into the water of both plots at the beginning of the season (1.1 kg N, 0.45 kg P, 0.45 kg K each per plot). Water was added to the well-watered plot when necessary to maintain a flood throughout the whole season.

Both plots were kept flooded with several cm of water for 3 weeks, and then the drought plot was drained and a part of the levee removed to ensure that water would drain out. The drought plot was not covered to keep out rain but rather remained uncovered to best simulate real-life conditions. The plot was on a very slight slope, so the open levee on the downslope side of the plot ensured that water would drain from the plot if it rained.

Gas exchange and chlorophyll fluorescence were measured using the LI-6400XT-40. Conditions in the measuring chamber were set to mimic ambient temperature, light, and vapor pressure deficit. Reference CO₂ levels were set to 400 ppm. Plants were measured both before the drought started to establish baseline photosynthesis and fluorescence and at periodic intervals of soil moisture to capture symptoms of progressive drought and create the drought response curve. Measurements were made between 8:00 AM and 1:00 PM, and we alternated the order the plants were measured to prevent time of measurement from severely affecting the data.

Soil moisture was first measured when the fields were saturated to set a baseline soil moisture level. Saturated volumetric soil moisture read at 50% with the soil moisture probe (Dynamax SM150 Portable Soil Moisture Probe, Dynamax, Fresno, CA, USA). The soil moisture probe was rods were 5.1 cm in length, meaning that the probe is not reading soil moisture throughout the entire depth of the rooting zone. The probe “reads” the soil moisture up to 2.5 cm in each direction from the center of the probe. We measured soil moisture daily once drought was induced, and gas exchange measurements began when the soil moisture was roughly

half of the saturated soil. For each LI-6400XT-40 measurement, we measured soil moisture at the base of each plant throughout the experiment.

2.3 Harvesting and Yield Evaluation

Rice plants were harvested when they were physiologically mature. Each plant was cut where it met the soil, and the entire plant was folded into a labeled paper bag and dried in an oven for one week. To determine yield, total panicles were counted on each plant and five representative panicles were selected from each plant. Panicle length was recorded, and total unfilled and filled grains were counted for each of the five selected panicles. We took an average of the five panicles to determine mean filled and unfilled grains per panicle for each plant.

2.4 Statistical Analysis

We used a Michaelis-Menten enzyme kinetic equation (Michaelis and Menten, 1913) in a multilevel Bayesian (MB) framework to estimate model parameters and associated uncertainties in different genotypes under a drought environment. The multilevel Bayesian Drought Response Curve (MBDRC) model has three primary components: (1) the likelihood model, which describes the likelihood of observed net photosynthesis (A_N), (2) the process model, which describes the photosynthesis response to soil moisture based on the Michaelis-Menten equation and process uncertainty associated with random effects, and (3) the prior distributions for model parameters and variance terms. The posterior distribution of all model parameters was obtained by combining these three parts (Wikle, 2003).

The likelihood model: We assume that the observations of photosynthesis are normally distributed for each observation i ($i=1, 2, \dots, n$):

$$A_{N[i]} \sim \text{Normal}(\mu_{[i]}, \tau) \quad \text{Eq. 1}$$

The process model: The process model describes the mean photosynthesis (μ) based on the Michaelis-Menten model as follows:

$$\mu_{[i]} = \frac{A_{max[Plant[i]]\theta_{[i]}}}{PLA_{50[Plant[i]]+\theta_{[i]}}} \quad \text{Eq. 2}$$

where $[Plant[i]]$ indicates plant-level parameters. The Michaelis-Menten equation is an asymptotic model describing the relationship between mean photosynthesis ($\mu_{[i]}$) and volumetric soil moisture (θ , %), where the horizontal asymptote ($X \rightarrow \infty$) is represented by A_{max} (maximum photosynthesis rate, $\mu\text{mol m}^{-2} \text{s}^{-1}$) and PLA_{50} is the θ level at which photosynthesis is 50% of A_{max} .

The parameter model: Two unknown plant level parameters of interest (A_{max} and PLA_{50}) are allowed to vary by each of the genotypes ($\mu.Parameter[s]$) ($s=1, 2, \dots, n$), where s indicates the number of genotypes. For example, genotype-level parameters are described as:

$$Parameter_{[s]} \sim Normal(\mu.Parameter, \tau.Parameter) \quad \text{Eq. 3}$$

where $\tau.Parameter$ is the precision (1/variance) term associated with the genotype-level mean ($\mu.Parameter$) of the parameter of interest. Parameters α and PLA_{50} were given informative prior distributions with posterior means normally distributed around a mean of zero and large standard deviation associated with them.

The observed likelihood, process, and parameter models were combined to generate the posterior distributions of the unknown parameters (Wikle, 2003). The joint posterior was sampled by implementing the Markov Chain Monte Carlo (MCMC) algorithms (Robert and Casella, 2009) in the Bayesian statistical software package WinBUGS (Lunn et al., 2000) by running three parallel MCMC chains. Each MCMC chain was run for 100,000 iterations after convergence and the BGR diagnostic tool was used to evaluate convergence of the chains to the posterior distribution (Brooks and Gelman, 1998). The chains were thinned every 10th iteration to

obtain an independent sample of 10,000 values per chain (total of 30,000 values) for each parameter from the joint posterior distribution. Model goodness-of-fit was evaluated by using Eq. 1 to generate modeled data for each observed photosynthesis value (Gelman et al., 2021) yielding posterior predictive distributions for each observation. The predicted means of photosynthesis with 95% credible intervals were compared with observed photosynthesis for evaluating the goodness-of-fit of the MBLRC model (see Appendix 1 for parameter estimates)

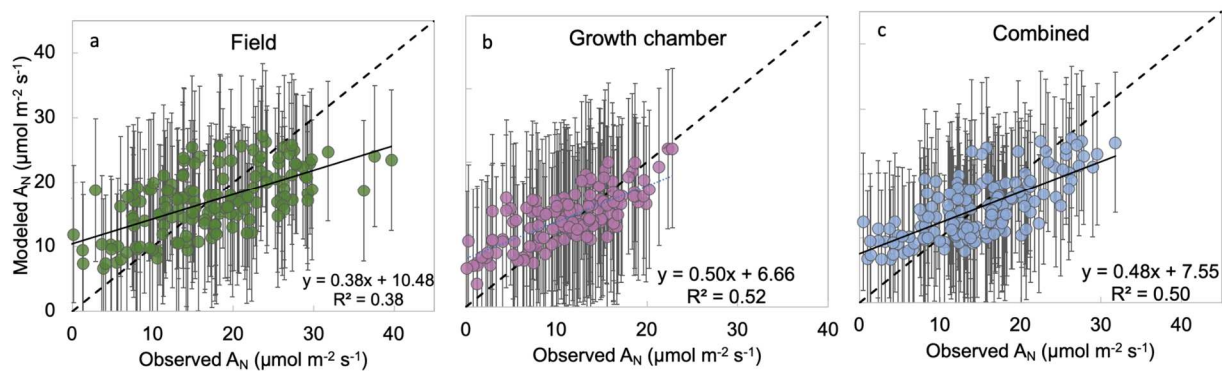


Figure 2. Relationship between observed and modeled values of the net photosynthesis rate (A_N , $\mu\text{mol m}^{-2} \text{s}^{-1}$) showing the model goodness-of-fit across growing environments. Error bars represent 2.5% (bottom) and 97.5% (top) credible intervals. The dotted line represents 1:1 line and the solid black line represents the linear fit to the data.

3. RESULTS

3.1 Model Goodness-of-Fit

The MBLRC model showed good ($R^2 = 0.50$) agreement between observed and modeled net photosynthesis rates (A_N), but consistently overestimated mean A_N at low values and underestimated mean A_N at higher values in both environments. (Figure 2). However, the observed data was within the range of the 95% credible interval (Figure 2). Across different

growing conditions, the model performed better in the growth chamber ($R^2 = 0.52$) than the field ($R^2 = 0.38$).

3.2 Developing a mechanistic model for photosynthesis response to drought

We developed a mechanistic model to describe the photosynthesis response of rice to progressive drought. The two parameters have biological meaning, where A_{max} represents maximum gross photosynthesis ($\mu\text{mol m}^{-2} \text{s}^{-1}$), and PLA_{50} is the volumetric soil water content (%) when photosynthesis is 50% of A_{max} . We hypothesized that the PLA_{50} parameter can be used to phenotype drought sensitivity of different genotypes and also used in crop models to improve prediction of photosynthesis under different environments. Genotypes with a higher sensitivity to drought will have a higher PLA_{50} value, indicating that photosynthesis declined to 50% of its maximum value at a greater soil moisture.

To determine whether photosynthesis response to drought can be predicted by a model, we subjected three rice genotypes (310723, 310588, and 311795) to progressive drought under controlled conditions in a growth chamber and monitored the photosynthesis response. The results are shown in Figure 3. Volumetric water content (θ) ranged from $\sim 3\%$ up to $\sim 40\%$ for each genotype, and there was a linear decline in net photosynthesis rate (A_N) when θ was around 10%.

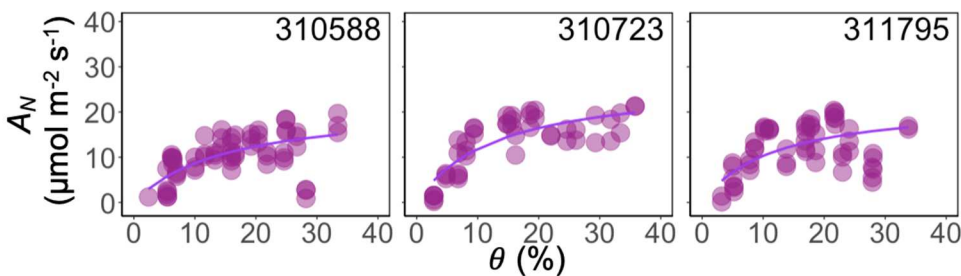


Figure 3. Photosynthesis (A_N , $\mu\text{mol m}^{-2} \text{s}^{-1}$) response to changing volumetric soil water content (θ) in (a) 310588, (b) 310723, and (c) 311795. Purple line is the model fit ($A_N = A_{max}\theta/(PLA_{50} +$

θ), where A_{max} is maximum photosynthesis rate ($\mu\text{mol m}^{-2} \text{s}^{-1}$), and PLA_{50} is the θ value when A_{max} is 50% indicating percent loss of assimilation (PLA).

3.3 Effect of growing conditions on photosynthesis response to drought

Our second objective was to understand whether the A_{max} and PLA_{50} parameters differed between a field environment and growth chamber pots. A_{max} was not significantly different between environments except in 310588 and 311795 (Figure 4). PLA_{50} in the field was significantly different from PLA_{50} in the growth chamber in 310588, 311677, N22, and ZHE, suggesting that this parameter may be more greatly influenced by environment than A_{max} , under drought conditions. Only in 310723 were neither parameter significantly different between environments.

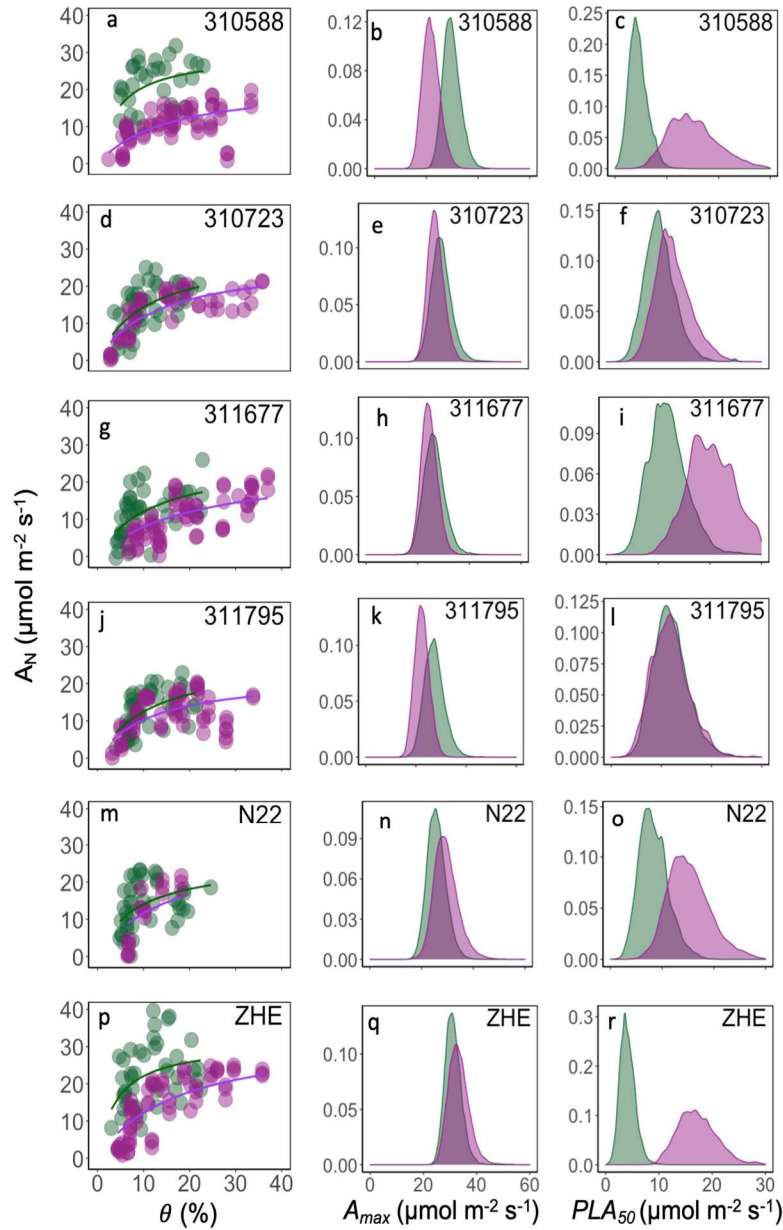


Figure 4. Photosynthetic drought response curves (a,d,g,j,m,p) and posterior density distribution of photosynthesis model parameters A_{max} ($\mu\text{mol m}^{-2} \text{s}^{-1}$) and PLA_{50} (%) for six rice (*Oryza sativa*) genotypes under field (green) and growth chamber (pink) conditions. Green and pink lines are the fit of a Michaelis-Menten model ($A_N = A_{max} * \theta / (PLA_{50} + \theta)$, where A_{max} is maximum photosynthesis rate ($\mu\text{mol m}^{-2} \text{s}^{-1}$), θ is volumetric soil water content (%), and PLA_{50} is θ at 50% of A_{max} for field and growth chamber plants, respectively).

3.4 Genotypic differences in photosynthesis response to drought

The model prediction showed good agreement with observed data when growth chamber and field data were combined in a hierarchical model (Figure 2c). Using this combined data, we evaluated the photosynthesis response across eight genotypes (Figure 5). 311677 had the highest PLA_{50} parameter value and was significantly different from all genotypes except 311795 and N22. 311792 was the least sensitive genotype and was significantly different from all genotypes except ZHE and 311620. A_{max} parameters were mostly similar across genotypes, except 311792 was significantly different from 310588, 310723, 311795, and ZHE. ZHE was significantly different from 311677, N22, and 311620, and 310588 was significantly different from 311620.

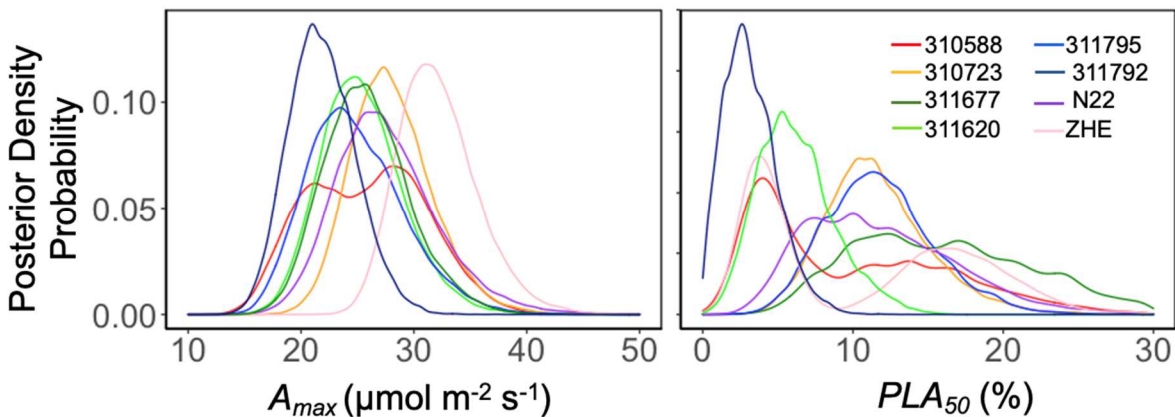


Figure 5. Posterior probability distributions for PLA_{50} (%) and A_{max} ($\mu\text{mol m}^{-2} \text{s}^{-1}$) of each genotype.

Our results show a negative correlation between PLA_{50} and plant yield (Figure 6); yield was smaller in plants that had a larger PLA_{50} parameter (higher sensitivity to drought), and was larger in genotypes with a smaller PLA_{50} parameter (lower sensitivity to drought). A weak positive relationship existed between yield and the A_{max} model parameter, however, there is a stronger positive relationship when 310588 and 311792 were removed from the relationship.

These two genotypes have a lower sensitivity to drought, and thus, even when photosynthesis has decreased due to drought, they are still capable of maintaining yield.

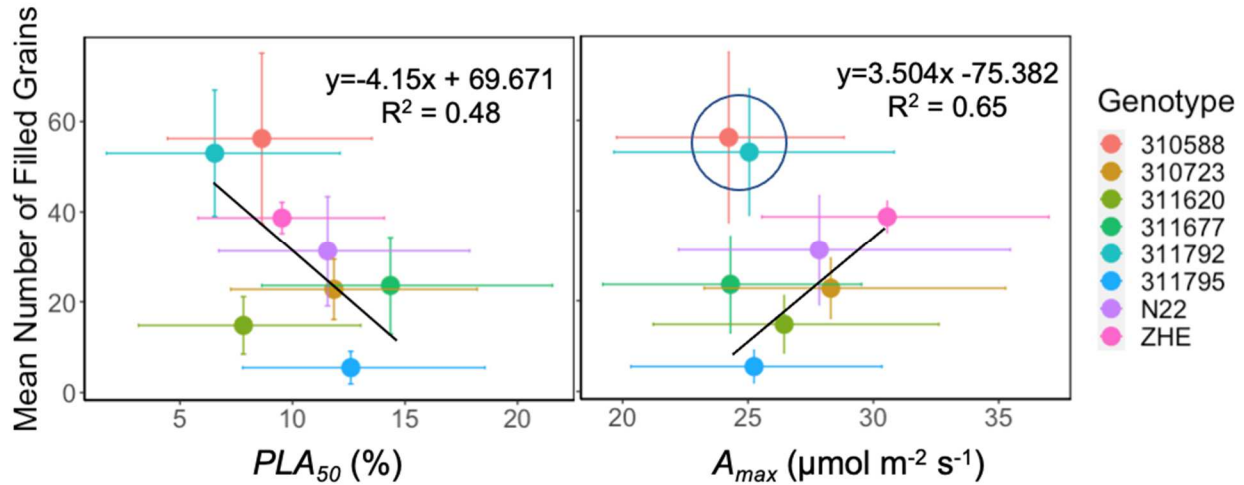


Figure 6. Relationship between the PLA_{50} (%) and A_{max} ($\mu\text{mol m}^{-2} \text{s}^{-1}$) model parameters of field and growth chamber plants and mean number of filled grains per panicle of field plants. Error bars on PLA_{50} are 95% credible intervals and error bars around mean number of filled grains are standard error about the mean. Data in the circle are less sensitive to drought and were not included in the regression.

4. DISCUSSION

We developed and tested a new model to phenotype drought sensitivity of crops and to predict yield under drought stress in eight different rice genotypes. We first tested the MBDR model in controlled conditions before expanding the tests to the field (Figure 2, Figure 4). The dynamic nature of the field environment makes evaluation of instantaneous point measurements of photosynthesis difficult in the field (Gu et al., 2012; Mishra et al., 2012; Tian-gen et al., 2017). However, phenotypic data from field trials may be more representative of real-life scenarios, and plant responses in controlled environments like greenhouses and growth chambers cannot always be transferred to the field (Langstroff et al., 2021). Plants do not grow in isolation

from their environment and the plasticity of plants under changing environmental conditions can produce a range of phenotypes (Pieruschka and Schurr, 2019). The phenotype of a plant is not only the expression of genes but the complex interactions with the internal and external environment as well (Trewavas and Malho, 1997; Sultan, 2000). It is not advisable to grossly extrapolate the results of either field or lab studies to environments outside of those in the experiment without careful consideration of both the study environment and the future environment (Tian-gen et al., 2017; Langstroff et al., 2021). However, the overlap of both the field and controlled environments presented here provides insights into the dynamic and intrinsic characteristics of these genotypes and contribute to models of future climate scenarios.

We quantified sensitivity to drought with the PLA_{50} parameter, soil moisture level at which plant photosynthesis decreased to half of its maximum photosynthesis. Figure 7 depicts the order of sensitivity to drought of the eight genotypes assessed in this study. 311677 and 311795 were found to be the most sensitive, while 311792 and 311620 were the least sensitive. Little is known in the literature about 311677, but 311795 has been studied and found to be generally sensitive to drought (Degenkolbe et al., 2009; Henry et al., 2011; Kumar, 2017). This is good confirmation that our model is operating well and identifying drought sensitivity accurately. N22 is another more well-studied genotype. It has been found to be drought tolerant (Degenkolbe et al., 2009; Kumar, 2017; Poli et al., 2018), though our model ranked it as moderately sensitive. However, PLA_{50} of N22 was significantly different between environments; N22 was significantly less sensitive in the field compared with the growth chamber. This emphasizes the necessity of evaluating stress response in a range of environments. ZHE tends to be a sensitive genotype to other kinds of stress (Moldenhauer et al., 2020) but was found to be only moderately sensitive to drought in this study. One reason for this could be this genotype's

exceptionally quick time to flowering. All of the plants were grown, planted, and subjected to drought at the same time. It is likely that ZHE was able to grow quickly and begin setting seed before it was severely affected by drought, presenting an appearance of resistance (high yield and low PLA_{50}) to drought through drought avoidance.

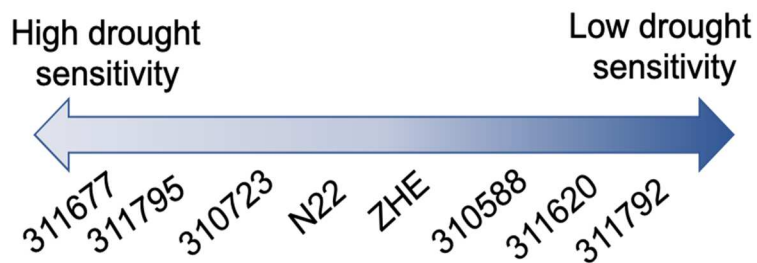


Figure 7. Drought sensitivity ranking of the eight genotypes selected for this work based on the multilevel Bayesian drought response curve model.

PLA_{50} in several genotypes was significantly different in growth chamber pots compared with the field environment (Figure 4). To cope with drought stress, many plants grow longer roots to reach water at deeper soil depths (Kato et al., 2006; Farooq et al., 2009). Plants in pots do not have the option to find deeper water. Across all genotypes, PLA_{50} was greater (though not always significantly) in the field plants compared with the growth chamber plants. It is possible that the genotypes that were able to continue photosynthesizing longer in the field (310588, N22, ZHE, 311677) coped with drought by growing longer roots to reach deeper soil water, while their counterparts in the growth chamber were unable to do so. Future research could examine the rooting depth and root architecture of these genotypes under drought stress in the field to determine which plants cope with drought stress by searching for water at greater depths. This emphasizes the importance of phenotyping for stress responses in field environments to accurately quantify phenotypic response to that stress.

The mean PLA_{50} for these genotypes ranged from 6-14%. This threshold is consistent with soil moisture of the permanent wilting point, where plant roots are unable to extract enough water to meet their demand, and plant processes, such as transpiration, cease (Cornell, 2010; Datta et al., 2018). Permanent wilting point ranges from 8% to 24% soil moisture in sand and clay soils, respectively (Cornell, 2010; Datta et al., 2018), and with our loamy soil type, we see that threshold generally falling within that range. Permanent wilting point is the point at which the plant does not recover turgor upon rewetting (Cornell, 2010), yet all of our plants recovered and grew to maturity. It is likely, then, that the soil moisture at a greater depth had not yet reached the permanent wilting point, allowing the plants to recover. Nevertheless, this genotype-specific threshold can be used as an indicator of plant photosynthetic status and correlation with yield

5. CONCLUSIONS

We developed and tested a novel mechanistic model in a probabilistic framework to phenotype and predict photosynthesis and yield response to drought under controlled and field conditions. This two-parameter (A_{max} and PLA_{50}) Michaelis-Menten model showed a good fit for predicting photosynthesis and yield response to drought in all genotypes across controlled and field conditions. The PLA_{50} parameter is an indicator of sensitivity, where a larger PLA_{50} value correlated with higher sensitivity to drought, and a smaller PLA_{50} value indicated low sensitivity to drought. Our results demonstrate the validity of this method to phenotype drought sensitivity using field generated yield data and good agreement with prior studies of genotype with known sensitivity to drought.

6. REFERENCES

- Amthor, J. S. (2007). "Improving photosynthesis and yield potential," in *Improvement of Crop Plants for Industrial End Uses*, ed. P. RANALLI (Dordrecht: Springer Netherlands), 27–58. doi:10.1007/978-1-4020-5486-0_2.
- Araus, J. L., and Cairns, J. E. (2014). Field high-throughput phenotyping: the new crop breeding frontier. *Trends in Plant Science* 19, 52–61. doi:10.1016/j.tplants.2013.09.008.
- Ba Hoang, T., and Kobata, T. (2009). Stay-Green in Rice (*Oryza sativa* L.) of Drought-Prone Areas in Desiccated Soils. *Plant Production Science* 12, 397–408. doi:10.1626/pp.s.12.397.
- Babar, M. A., Reynolds, M. P., Ginkel, M. van, Klatt, A. R., Raun, W. R., and Stone, M. L. (2006). Spectral Reflectance to Estimate Genetic Variation for In-Season Biomass, Leaf Chlorophyll, and Canopy Temperature in Wheat. *Crop Science* 46, 1046–1057. doi:10.2135/cropsci2005.0211.
- Bailey-Serres, J., Parker, J. E., Ainsworth, E. A., Oldroyd, G. E. D., and Schroeder, J. I. (2019). Genetic strategies for improving crop yields. *Nature* 575, 109–118. doi:10.1038/s41586-019-1679-0.
- Beverly, D. P., Guadagno, C. R., and Ewers, B. E. (2020). Biophysically Informed Imaging Acquisition of Plant Water Status. *Frontiers in Forests and Global Change* 3, 125. doi:10.3389/ffgc.2020.589493.
- Brooks, S. P., and Gelman, A. (1998). General Methods for Monitoring Convergence of Iterative Simulations. *Journal of Computational and Graphical Statistics* 7, 434–455. doi:10.1080/10618600.1998.10474787.
- Caine, R. S., Yin, X., Sloan, J., Harrison, E. L., Mohammed, U., Fulton, T., et al. (2018). Rice with reduced stomatal density conserves water and has improved drought tolerance under future climate conditions. *New Phytologist* 0. doi:10.1111/nph.15344.
- Cornell (2010). Soil hydrology AEM. *Northeast Region Certified Crop Advisor study resources*. Available at: <https://nrcca.cals.cornell.edu/soil/CA2/CA0212.1-3.php> [Accessed November 23, 2021].
- Costa, C., Schurr, U., Loreto, F., Menesatti, P., and Carpentier, S. (2019). Plant Phenotyping Research Trends, a Science Mapping Approach. *Front. Plant Sci.* 9. doi:10.3389/fpls.2018.01933.
- Cruz, J. A., Savage, L. J., Zegarac, R., Hall, C. C., Satoh-Cruz, M., Davis, G. A., et al. (2016). Dynamic environmental photosynthetic imaging reveals emergent phenotypes. *Cell Systems* 2, 365–377. doi:10.1016/j.cels.2016.06.001.

- Datta, S., Taghveian, S., and Stivers, J. (2018). Understanding Soil Water Content and Thresholds for Irrigation Management. Oklahoma State University Extension Available at: <https://extension.okstate.edu/fact-sheets/understanding-soil-water-content-and-thresholds-for-irrigation-management.html> [Accessed November 10, 2021].
- Deery, D. M., Rebetzke, G. J., Jimenez-Berni, J. A., James, R. A., Condon, A. G., Bovill, W. D., et al. (2016). Methodology for High-Throughput Field Phenotyping of Canopy Temperature Using Airborne Thermography. *Frontiers in Plant Science* 7, 1808. doi:10.3389/fpls.2016.01808.
- Degenkolbe, T., Do, P. T., Zuther, E., Repsilber, D., Walther, D., Hinch, D. K., et al. (2009). Expression profiling of rice cultivars differing in their tolerance to long-term drought stress. *Plant Mol Biol* 69, 133–153. doi:10.1007/s11103-008-9412-7.
- Farooq, M., Wahid, A., Lee, D.-J., Ito, O., and Siddique, K. H. M. (2009). Advances in drought resistance of rice. *Critical Reviews in Plant Sciences* 28, 199–217. doi:10.1080/07352680902952173.
- Farquhar, G., von Caemmerer, S., and Berry, J. (1980). *A biochemical model of photosynthetic CO₂*. doi:10.1007/BF00386231.
- Fiorani, F., and Schurr, U. (2013). Future Scenarios for Plant Phenotyping. *Annual Review of Plant Biology* 64, 267–291. doi:10.1146/annurev-arplant-050312-120137.
- Furbank, R. T., and Tester, M. (2011). Phenomics – technologies to relieve the phenotyping bottleneck. *Trends in Plant Science* 16, 635–644. doi:10.1016/j.tplants.2011.09.005.
- Gelman, A., Carlin, J. B., Stern, H. S., Dunson, D. B., Vehtari, A., and Rubin, D. B. (2021). *Bayesian Data Analysis*. 677.
- Ghanem, M. E., Marrou, H., and Sinclair, T. R. (2015). Physiological phenotyping of plants for crop improvement. *Trends in Plant Science* 20, 139–144. doi:10.1016/j.tplants.2014.11.006.
- Gu, J., Yin, X., Struik, P. C., Stomph, T. J., and Wang, H. (2012). Using chromosome introgression lines to map quantitative trait loci for photosynthesis parameters in rice (*Oryza sativa* L.) leaves under drought and well-watered field conditions. *Journal of Experimental Botany* 63, 455–469. doi:10.1093/jxb/err292.
- Hai, N. N., Chuong, N. N., Tu, N. H. C., Kisiala, A., Hoang, X. L. T., and Thao, N. P. (2020). Role and Regulation of Cytokinins in Plant Response to Drought Stress. *Plants (Basel)* 9, 422. doi:10.3390/plants9040422.
- Han, M.-L., Lv, Q.-Y., Zhang, J., Wang, T., Zhang, C.-X., Tan, R.-J., et al. (2021). Decreasing nitrogen assimilation under drought stress by suppressing DST-mediated activation of

- Nitrate Reductase 1.2 in rice. *Mol Plant*, S1674-2052(21)00365–8.
doi:10.1016/j.molp.2021.09.005.
- Henry, A., Gowda, V. R. P., Torres, R. O., McNally, K. L., and Serraj, R. (2011). Variation in root system architecture and drought response in rice (*Oryza sativa*): Phenotyping of the OryzaSNP panel in rainfed lowland fields. *Field Crops Research* 120, 205–214.
doi:10.1016/j.fcr.2010.10.003.
- Herrmann, H. A., Schwartz, J.-M., and Johnson, G. N. (2019). From empirical to theoretical models of light response curves - linking photosynthetic and metabolic acclimation. *Photosynth Res.* doi:10.1007/s11120-019-00681-2.
- Jones, H. G., Serraj, R., Loveys, B. R., Xiong, L., Wheaton, A., Price, A. H., et al. (2009). Thermal infrared imaging of crop canopies for the remote diagnosis and quantification of plant responses to water stress in the field. *Functional Plant Biol.* 36, 978–989.
doi:10.1071/FP09123.
- Kamoshita, A., Babu, R. C., Boopathi, N. M., and Fukai, S. (2008). Phenotypic and genotypic analysis of drought-resistance traits for development of rice cultivars adapted to rainfed environments. *Field Crops Research* 109, 1–23. doi:10.1016/j.fcr.2008.06.010.
- Kato, Y., Kamoshita, A., Yamagishi, J., and Abe, J. (2006). Growth of three rice (*Oryza sativa* L.) cultivars under upland conditions with different levels of water supply. *Plant Production Science* 9, 422–434. doi:10.1626/ppp.9.422.
- Kissoudis, C., van de Wiel, C., Visser, R. G., and van der Linden, G. (2016). Future-proof crops: challenges and strategies for climate resilience improvement. *Current Opinion in Plant Biology* 30, 47–56. doi:10.1016/j.pbi.2016.01.005.
- Kitomi, Y., Hanzawa, E., Kuya, N., Inoue, H., Hara, N., Kawai, S., et al. (2020). Root angle modifications by the DRO1 homolog improve rice yields in saline paddy fields. *PNAS* 117, 21242–21250. doi:10.1073/pnas.2005911117.
- Kumar, A. (2017). Development and characterization of rice genotypes for water use efficiency and drought resistance. *ProQuest Dissertations and Theses*. Available at: <https://www.proquest.com/docview/2317708251/abstract/CDE662A53F2C4753PQ/1> [Accessed October 30, 2021].
- Langstroff, A., Heuermann, M. C., Stahl, A., and Junker, A. (2021). Opportunities and limits of controlled-environment plant phenotyping for climate response traits. *Theor Appl Genet.* doi:10.1007/s00122-021-03892-1.
- Lunn, D. J., Thomas, A., Best, N., and Spiegelhalter, D. (2000). WinBUGS - A Bayesian modelling framework: Concepts, structure, and extensibility. *Statistics and Computing* 10, 325–337.

- Medlyn, B. E., Dreyer, E., Ellsworth, D., Forstreuter, M., Harley, P. C., Kirschbaum, M. U. F., et al. (2002). Temperature response of parameters of a biochemically based model of photosynthesis. II. A review of experimental data. *Plant, Cell & Environment* 25, 1167–1179. doi:10.1046/j.1365-3040.2002.00891.x.
- Michaelis, L., and Menten, M. L. (1913). The kinetics of invertase action. *Z* 49, 333–369.
- Mishra, Y., Johansson Jänkänpää, H., Kiss, A. Z., Funk, C., Schröder, W. P., and Jansson, S. (2012). Arabidopsis plants grown in the field and climate chambers significantly differ in leaf morphology and photosystem components. *BMC Plant Biology* 12, 6. doi:10.1186/1471-2229-12-6.
- Mohanty, S., Wassmann, R., Nelson, A., Moya, P., and Jagadish, S. V. K. (2013). Rice and climate change: significance for food security and vulnerability. *IRRI Discussion Paper Series No. 49*, 18.
- Moldenhauer, K., Scott, B., and Harke, J. (2020). B.R. Wells Arkansas Rice Research Studies 2019. 270.
- Pieruschka, R., and Schurr, U. (2019). Plant phenotyping: past, present, and future. *Plant Phenomics*. doi:10.34133/2019/7507131.
- Pinheiro, C., and Chaves, M. M. (2011). Photosynthesis and drought: can we make metabolic connections from available data? *Journal of Experimental Botany* 62, 869–882. doi:10.1093/jxb/erq340.
- Poli, Y., Balakrishnan, D., Desiraju, S., Panigrahy, M., Voleti, S. R., Mangrauthia, S. K., et al. (2018). Genotype × Environment interactions of Nagina22 rice mutants for yield traits under low phosphorus, water limited and normal irrigated conditions. *Sci Rep* 8, 15530. doi:10.1038/s41598-018-33812-1.
- Robert, C. P., and Casella, G. (2009). Introducing Monte Carlo Methods with R. 239.
- Sass, L., Majer, P., and Hideg, E. (2012). Leaf hue measurements: a high-throughput screening of chlorophyll content. *Methods Mol Biol* 918, 61–69. doi:10.1007/978-1-61779-995-2_6.
- Searchinger, T., Waite, R., Hanson, C., and Ranganathan, J. (2019). Creating a sustainable food future: a menu of solutions to feed nearly 10 billion people by 2050. World Resources Institute Available at: https://research.wri.org/sites/default/files/2019-07/WRR_Food_Full_Report_0.pdf [Accessed February 12, 2021].
- Shahbandeh, M. (2019). Grain production worldwide by type, 2018/19. *Statista*. Available at: <https://www.statista.com/statistics/263977/world-grain-production-by-type/> [Accessed January 24, 2020].

- Sharkey, T. D., Bernacchi, C. J., Farquhar, G. D., and Singaas, E. L. (2007). Fitting photosynthetic carbon dioxide response curves for C3 leaves. *Plant, Cell & Environment* 30, 1035–1040. doi:10.1111/j.1365-3040.2007.01710.x.
- Silva-Perez, V., Molero, G., Serbin, S. P., Condon, A. G., Reynolds, M. P., Furbank, R. T., et al. (2018). Hyperspectral reflectance as a tool to measure biochemical and physiological traits in wheat. *J Exp Bot* 69, 483–496. doi:10.1093/jxb/erx421.
- Simkin, A. J., López-Calcagno, P. E., and Raines, C. A. (2019). Feeding the world: improving photosynthetic efficiency for sustainable crop production. *J Exp Bot* 70, 1119–1140. doi:10.1093/jxb/ery445.
- Sinclair, T. R., Purcell, L. C., and Sneller, C. H. (2004). Crop transformation and the challenge to increase yield potential. in *Trends in Plant Science. Vol.9 No.2*.
- Sultan, S. E. (2000). Phenotypic plasticity for plant development, function and life history. *Trends in Plant Science* 5, 537–542. doi:10.1016/S1360-1385(00)01797-0.
- Tackenberg, O. (2007). A New Method for Non-destructive Measurement of Biomass, Growth Rates, Vertical Biomass Distribution and Dry Matter Content Based on Digital Image Analysis. *Annals of Botany* 99, 777–783. doi:10.1093/aob/mcm009.
- Tessmer, O. L., Jiao, Y., Cruz, J. A., Kramer, D. M., and Chen, J. (2013). Functional approach to high-throughput plant growth analysis. *BMC Syst Biol* 7, S17. doi:10.1186/1752-0509-7-S6-S17.
- Thornley, J. H. M., and Johnson, I. R. (1990). *Plant and Crop Modeling*. Oxford: University Press.
- Tian-gen, C., Chang-peng, X., Ming-nan, Q., Hong-long, Z., Qing-feng, S., and Xin-guang, Z. (2017). Evaluation of protocols for measuring leaf photosynthetic properties of field-grown rice. *Rice Science* 24, 1–9. doi:10.1016/j.rsci.2016.08.007.
- Trewavas, A., and Malho, R. (1997). Signal Perception and Transduction: The Origin of the Phenotype. *Plant Cell* 9, 1181–1195.
- Tuberosa, R. (2012). Phenotyping for drought tolerance of crops in the genomics era. *Front. Physiol.* 0. doi:10.3389/fphys.2012.00347.
- USDA Web Soil Survey. Available at: <https://websoilsurvey.sc.egov.usda.gov/App/WebSoilSurvey.aspx> [Accessed November 10, 2021].
- Varshney, R. K., Graner, A., and Sorrells, M. E. (2005). Genomics-assisted breeding for crop improvement. *Trends in Plant Science* 10, 621–630. doi:10.1016/j.tplants.2005.10.004.
- Wang, Z., Li, G., Sun, H., Ma, L., Guo, Y., Zhao, Z., et al. (2018). Effects of drought stress on

- photosynthesis and photosynthetic electron transport chain in young apple tree leaves. *Biol Open* 7, bio035279. doi:10.1242/bio.035279.
- Wikle, C. K. (2003). Hierarchical Models in Environmental Science. *International Statistical Review* 71, 181–199. doi:10.1111/j.1751-5823.2003.tb00192.x.
- Wu, A., Hammer, G. L., Doherty, A., von Caemmerer, S., and Farquhar, G. D. (2019). Quantifying impacts of enhancing photosynthesis on crop yield. *Nat. Plants* 5, 380–388. doi:10.1038/s41477-019-0398-8.
- Yang, X., Wang, B., Chen, L., Li, P., and Cao, C. (2019). The different influences of drought stress at the flowering stage on rice physiological traits, grain yield, and quality. *Scientific Reports* 9, 1–12. doi:10.1038/s41598-019-40161-0.
- Zargar, S. M., Gupta, N., Nazir, M., Mahajan, R., Malik, F. A., Sofi, N. R., et al. (2017). Impact of drought on photosynthesis: Molecular perspective. *Plant Gene* 11, 154–159. doi:10.1016/j.plgene.2017.04.003.
- Zuluaga, A. P., Bidzinski, P., Chanclud, E., Ducasse, A., Cayrol, B., Gomez Selvaraj, M., et al. (2020). The Rice DNA-Binding Protein ZBED Controls Stress Regulators and Maintains Disease Resistance After a Mild Drought. *Frontiers in Plant Science* 11, 1265. doi:10.3389/fpls.2020.01265.

CHAPTER 3: Effects of Growing Conditions and Measurement Methods on Phenotypic Expression of Photosynthesis

ABSTRACT

Photosynthesis light response curves are widely used to quantify phenotypic expression of photosynthesis including the maximum photosynthetic capacity (A_{max}), apparent quantum yield (α), and mitochondrial respiration (R_d) in response to changing environmental conditions. Two common methods of generating these curves involve measuring photosynthesis (1) on a single sample by sequentially altering the intensity of light within a chamber (sequential method), or (2) on samples that are each equilibrated to a different light level (non-sequential method), eliminating the dosage effects of sequential light response curves. Both methods are often conducted in controlled environments to achieve steady-state results and neither method involves equilibrating the entire plant to the specific light level. Here, we compare sequential and non-sequential methods for generating light response curves in controlled (greenhouse), semi-controlled (plant grown in growth chamber and acclimated to field conditions 2-3 day before measurements), and field conditions. We selected seven different rice genotypes for this experiment with overarching goals to understand (1) phenotypic plasticity of rice grown under different environments, and (2) the limitations of different methods of generating light response curves. We used the non-rectangular hyperbola model in a hierarchical Bayesian framework to estimate model parameters and associated uncertainties for comparison across methods and growing conditions. Our results show that A_{max} is significantly lower across all genotypes under greenhouse conditions compared to the growth chamber and field conditions, while α , θ (shape parameter), and R_d were generally not significantly different among environments. The non-

sequential method generated light response curves that were similar to the sequential method, but took less time and accurately captured the variability of the field environment. The non-sequential method would be particularly useful to conduct curves on a large number of plants in less time under field conditions.

1. INTRODUCTION

Expected global temperature rise and water scarcity (IPCC 2019) present serious threats to crop production and global food security. To feed the growing human population without using more land while reducing water use and greenhouse gas emissions, we need to investigate the limitation of commonly used measurement and modeling techniques used for quantifying gene and environment interactions. Photosynthesis response (light, CO₂, and temperature) curves are commonly used to estimate species-specific parameters, including maximum photosynthetic capacity, maximum electron transport rate, mitochondrial respiration, maximum light use efficiency, maximum gross and net photosynthesis, and optimal temperature (Berry and Bjorkman, 1980; Farquhar et al., 1980; Battaglia et al., 1996; Medlyn et al., 2002; Ralph and Gademann, 2005; Lobo et al., 2013). These parameters provide insight into the intrinsic characteristics of the plants based on biological mechanisms. Understanding crop response to variable environmental conditions is critical to improve our predictions of crop yield that is often correlated with the plant biomass and photosynthesis (Zelitch, 1982; Bouman and Tuong, 2001). To meet the increasing demand of food (the global human population is expected to reach 9 billion by 2050) and adapt to a warming planet (global temperatures are expected to rise more than 2 °C by 2050 without deep emission reductions), predictive crop models based on

mechanistic understanding of photosynthesis response to changing environmental conditions are needed for selecting and breeding plants for desirable attributes.

Conventionally, photosynthesis light response curves are generated by clamping one or more leaves into a chamber and altering the level of the light intensity within the chamber of a gas exchange measurement system (e.g., LI-6400XT, Li-COR Biosciences, Lincoln, NE, USA and CIRAS-3, PP Systems, Amesbury, MA, USA) (McDermitt et al., 1989; Ögren, 1993; Dreyer et al., 2001; Medlyn et al., 2002; Sharkey et al., 2007). This method requires significant time for each curve, as plants need to acclimate for several minutes at each light level (Battaglia et al., 1996; Serôdio et al., 2013). Steady-state light response curves require 10-20 minutes at each light level to allow the plant to acclimatize to the current light level; this allows for characterization of the plasticity and inherent steady-state photosynthesis properties at different light intensities (Coe and Lin, 2018). Rapid light response curves can be generated more quickly, with only 1-3 minutes needed at each light level (Coe and Lin, 2018; LI-COR, 2021) and can be used to characterize the plant's dynamic photosynthetic response under rapidly fluctuating light conditions (Ralph and Gademann, 2005; Coe and Lin, 2018). Non-sequential (or survey) light response curves are similar to rapid sequential light response curves, but rather than subjecting the same sample to a sequence of light intensities, different samples, equilibrated at different light intensities, are used to build a similar curve (Perkins et al., 2006; Houliez et al., 2017; Coe and Lin, 2018; LI-COR, 2021). Non-sequential light response curves are often conducted on microalgae (Perkins et al., 2006), phytoplankton (Houliez et al., 2017), or other marine plants (Ralph and Gademann, 2005) using chlorophyll fluorescence parameter response to light rather than net photosynthesis.

In each of these methods for generating light response curves in land plants, a portion of a leaf is enclosed in an artificial environment, different from what the rest of the plant is experiencing. This difference between whole plant and measuring environment may limit the reliability of the conventional response curves to estimate the full photosynthetic capacity of the whole plant (Wagner and Reicosky, 1992; Sims et al., 1998). Additionally, most plants are measured in controlled environments, but recent studies demonstrating phenotypic plasticity of plants (Sultan, 2000; Pieruschka and Schurr, 2019) suggest that plant response under controlled environment conditions will likely differ from their response under field environments (Sultan, 2000). However, if the non-sequential light response curves are conducted in a field environment, sampling different leaves on plants that acclimate to light levels throughout the day, we ensure that the whole plant is equilibrated to the current light level and that the measurements reflect the real environment. This type of curve eliminates the effect of the previous light intensities on the current measurement (Coe and Lin, 2018) and has values that are equilibrated to the current light level (Coe and Lin, 2018; LI-COR, 2021).

Rice (*Oryza sativa*) is grown worldwide and supports more than half of the world's population as a primary food source (Mohanty et al., 2013). Here, we use different rice genotypes to understand the phenotypic plasticity of crops under different environments and the limitations of different methods. We asked: (1) do model (non-rectangular hyperbola model fitted to the photosynthesis light response curve) parameters under controlled conditions differ from the model parameters under field conditions? and (2) do model parameters vary between sequential and non-sequential methods of generating light response curves?

2. METHODS

2.1 Plant Material

Rice genotypes for all experiments in this research were selected from the USDA rice mini-core collection, which is a collection of 217 genotypes with diverse origins, subgroups, and phenotypic and genotypic expressions (Agrama et al., 2009; Kumar, 2017). We selected seven of these genotypes to include in this research: 310588, 310723, 311677, 311795, Nagina 22 (N22), and Zhe733 (ZHE). Details of each of these genotypes are provided in Table 1.

Table 1. Information about rice genotypes used across different growing environments: F = field, GC = growth chamber, GH = greenhouse. Sequential and non-sequential light response curves were conducted on all genotypes.

USDA Accession Number	Genotype Name	Taxon	Subgroup	Country of Origin	Growing Environment
310588	Onu B	<i>Oryza sativa</i>	TRJ	Zaire	F, GC, GH
310723	WIR 3039	<i>Oryza sativa</i>	AUS	Tajikistan	F, GC
311620	Romeno	<i>Oryza sativa</i>	TEF	Portugal	F, GC
311677	Karabaschak	<i>Oryza sativa</i>	TEJ	Bulgaria	F, GC
311792	Cypress	<i>Oryza sativa</i>	TRJ	United States	F, GC
311795	Nipponbare	<i>Oryza sativa</i>	TEJ	Japan	F, GC, GH
	Nagina 22	<i>Oryza sativa</i>	AUS	India	F, GC, GH
	Zhe733	<i>Oryza sativa</i>	IND	China	F, GC

2.2 Photosynthesis Light Response Curve Measurements

2.2.1 Field Experiment

Five replicates of each genotype were germinated in pots and transplanted (21 day after germination) to a 6 x 6 m, levee-bound plot at the University of Arkansas Division of Agriculture's Agriculture Experiment Station in Fayetteville, AR (36.096051°, -94.167418°).

Plants were transplanted 0.3 m apart from each other in rows according to genotype with five replicates per genotype, a total of 35 plants. A flood of 2-10 cm was maintained on the field for the entire growing season of 2019. The field soils were a combination of Pembroke silt loam (fine-silty, mixed, active, mesic Mollic Paleudalfs) and Pickwick wilt loam (fine-silty, mixed, semiactive, thermic Typic Paleudults) (USDA).

Light response curves were generated *in situ* for plants grown in the field (Figure 1a) using the non-sequential survey method (Perkins et al., 2006; Houliez et al., 2017; Coe and Lin, 2018; LI-COR, 2021) where diurnal light intensities and multiple plant replicates were used to fully capture the variability and photosynthetic range within each genotype. These curves take advantage of the natural diurnal light pattern of the day and the photosynthetic response of the whole plant to those changing light levels to create the curve rather than altering the environment of a small portion of a leaf. For these curves, instantaneous measurements with the LI-6400XT began around 7 AM and were collected throughout the day on all replicates until 4-5 PM, or until three measurements on each plant were taken. A complete curve for a genotype has 15 data points (three measurements on five plants). Photosynthetically active radiation (PAR) and air temperature within the leaf chamber were set to reflect ambient PAR ($1-2400 \mu\text{mol m}^{-2} \text{s}^{-1}$), temperature (24-36 °C), and vapor pressure deficit (VPD, 0.79-3.5 kPa). Proper care was taken to ensure the sensor was not shaded by leaves or the researchers' bodies.

2.2.2 Growth Chamber Experiment

Growth chamber plants were germinated, three seeds to a 3.8 L pot, in a greenhouse, then moved to a growth chamber after 4 weeks. Soil medium was 5:1 potting soil to field soil. Lights

in the growth chamber were set to $600 \mu\text{mol m}^{-2} \text{s}^{-1}$ on a 14-10 light-dark cycle and temperature was set to around $28 \text{ }^{\circ}\text{C}$. Pots were watered daily to ensure adequate soil moisture.

These response curves combined the sequential response curve methodology of the greenhouse plants with the environment of the field plants. After growing for 3 weeks in the growth chamber, pots were moved outside into water-filled trays in the sunlight where they were allowed to acclimate for 2-3 days (Figure 1b). An auto-program (reference CO_2 set to 410 ppm, block temperature and VDP set to ambient ($26\text{-}40 \text{ }^{\circ}\text{C}$ and $1\text{-}4 \text{ kPa}$)) with 11 light levels ($2000, 1600, 1400, 1200, 1000, 800, 600, 400, 200, 50 \mu\text{mol m}^{-2} \text{s}^{-1}$) was then run on three plants of each genotype. The experiment was repeated for a total of three rounds, however, seeds for N22 only germinated for one round, so there are fewer replicates. Air temperature during measurements ranged from $24\text{-}38 \text{ }^{\circ}\text{C}$, with an average temperature of $33 \text{ }^{\circ}\text{C}$. Relative humidity was around 47%, and PAR often ranged between $1300\text{-}2300 \mu\text{mol m}^{-2} \text{s}^{-1}$ during measurements, taken between 11 AM -2 PM CST.

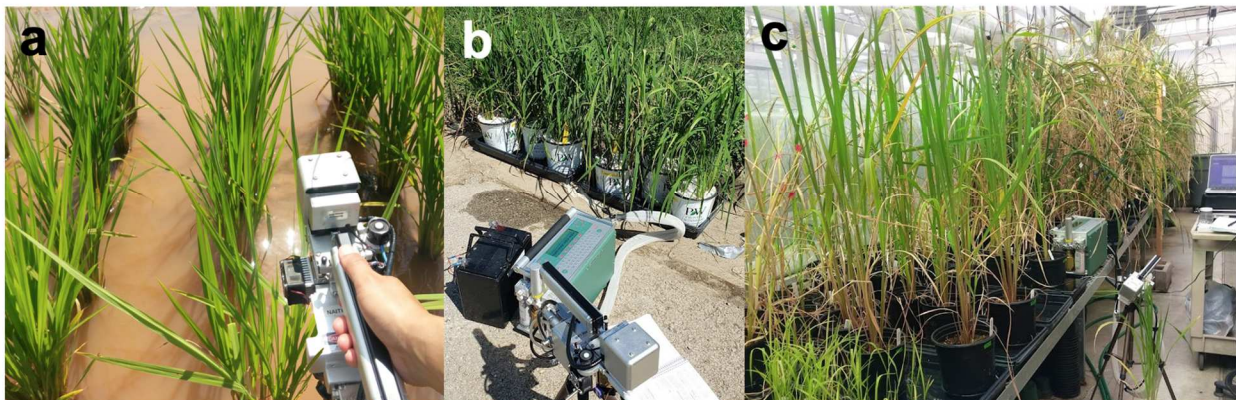


Figure 1. Images showing measurements of rice plants with the LI-6400XT across different growing environments including (a) field, (b) growth chamber-grown pots acclimated to field conditions, and (c) greenhouse conditions.

2.2.3. Greenhouse Experiment

Greenhouse studies were conducted in University of Arkansas's greenhouses in Fayetteville, AR (Figure 1c). Plants were grown in 0.95 L pots in trays of water to simulate flooded conditions. Pots were filled with mixed soil (five parts potting soil and one part autoclaved field soil). Field soils were collected from the same location as the field experiment was conducted. We used the sequential, rapid method of measuring photosynthesis response to light with an LI-6400XT (LI-COR Biosciences, Lincoln, NE, USA) on a healthy, mature leaf. An auto-program was created to collect data at 10 light levels (1400, 1200, 1000, 800, 600, 400, 200, 100, 50, 0 $\mu\text{mol m}^{-2} \text{s}^{-1}$) beginning at the highest light and allowing up to 3-minute of acclimation at each level.

2.3 Statistical Analysis

We used a non-rectangular hyperbola model (Thornley and Johnson, 1990; Thornley, 1998) in a multilevel Bayesian (MB) framework (Clark and Gelfand, 2006) to estimate model parameters and associated uncertainties in different genotypes and environments. The MBLRC (Multilevel Bayesian Light Response Curve) model has three primary components: (1) the likelihood model which describes the likelihood of the observed net photosynthesis rate (A_N), (2) the process model which describes the photosynthesis response to light (photosynthetically active radiation, PAR) based on the non-rectangular hyperbola model and process uncertainty associated with random effects, and (3) the prior distributions for model parameters and precision terms. The posterior distribution of all model parameters was obtained by combining these three parts (Wikle, 2003).

The likelihood model: We assume that the observations of photosynthesis are normally distributed for each observation i ($i = 1, 2, \dots n$):

$$A_{N[i]} \sim \text{Normal}(\mu_{[i]}\tau) \quad \text{Eq. 1}$$

The process model: The process model describes the mean photosynthesis (μ) based on the non-rectangular hyperbola model as follows:

$$\mu[i] = \frac{\alpha_{[Plant[i]]} \times PAR_{[i]} \times A_{max[Plant[i]]} - \sqrt{(\alpha_{[Plant[i]]} \times PAR_{[i]} + A_{max[Plant[i]])^2 - 4\theta_{[Plant[i]]} \times \alpha_{[Plant[i]]} + A_{max[Plant[i]]}}}{2\theta_{[Plant[i]]}} - R_{d[Plant[i]]} \quad \text{Eq. 2}$$

where $[Plant[i]]$ indicates plant-level parameters, A_{max} is maximum gross photosynthesis ($\mu\text{mol m}^{-2} \text{s}^{-1}$), α is the apparent quantum efficiency ($\mu\text{mol m}^{-2} \text{s}^{-1}$), R_d is mitochondrial respiration ($\mu\text{mol m}^{-2} \text{s}^{-1}$), and θ (unitless) is the shape parameter for the curve.

The parameter model: Four unknown parameters of interest (A_{max} , α , R_d , and θ) are allowed to vary by each of the seven genotypes ($\mu.\text{Parameter}[s]$) ($s=1, \dots n$), where s indicates the number of genotypes. For example, genotype-level parameters are described as:

$$\text{Parameter}_{[s]} \sim \text{Normal}(\mu.\text{Parameter}, \tau.\text{Parameter}) \quad \text{Eq. 3}$$

where $\tau.\text{parameter}$ is the precision (1/variance) term associated with the genotype-level mean ($\mu.\text{Parameter}$) of the parameter of interest. A_{max} , α , R_d , and θ were given informative prior distributions with posterior means normally distributed around a mean reported in published literature and large ($\pm 200\%$) variances associated with them.

The observed likelihood, process, and parameter models were combined to generate the posterior distributions of the unknown parameters (Wikle, 2003). The joint posterior was sampled by implementing the Markov Chain Monte Carlo (MCMC) algorithms (Robert and Casella) in the Bayesian statistical software package WinBUGS (Lunn et al., 2000) by running three parallel MCMC chains. Each MCMC chain was run for 10,000 iterations after convergence

and the BGR diagnostic tool was used to evaluate convergence of the chains to the posterior distribution (Brooks and Gelman, 1998). The chains were thinned every 10th iteration to obtain an independent sample of 10,000 values per chain (total of 30,000 values) for each parameter from the joint posterior distribution. Model goodness-of-fit was evaluated by using Eq. 1 to generate modeled data for the observed photosynthesis values (Gelman et al., 2021) yielding posterior predictive distributions for each observation. The predicted means of photosynthesis with 95% credible intervals were compared with observed photosynthesis for evaluating the model goodness-of-fit (see Appendix 1 for parameter estimates).

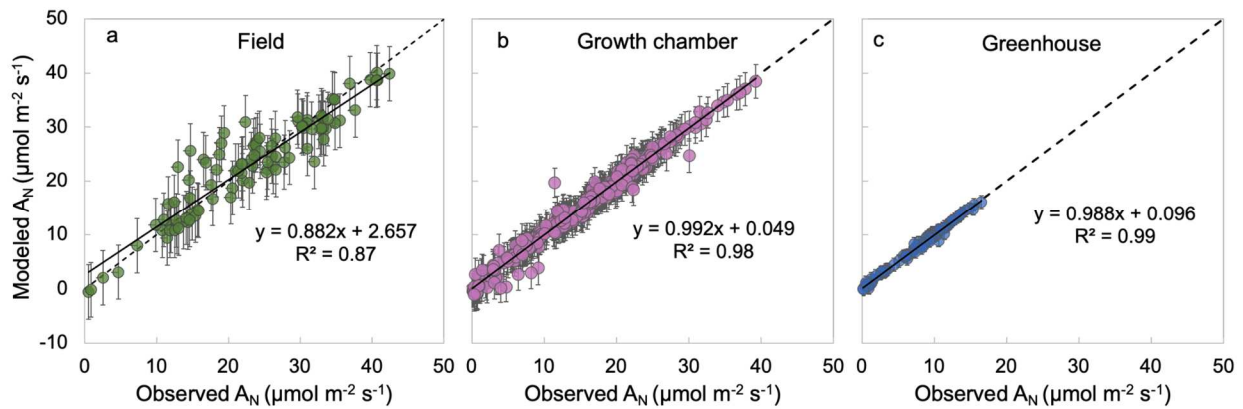


Figure 2. Relationship between observed and modeled values of the net photosynthesis rate (A_N , $\mu\text{mol m}^{-2} \text{s}^{-1}$) showing the model goodness-of-fit across different growing environments. Error bars represent 2.5% (bottom) and 97.5% (top) credible intervals. The dotted line represents 1:1 line and the solid black line represents the linear fit to the data.

For hypothesis testing ($\mu_1 - \mu_2 = 0$) differences in means were calculated by using `diffdist` function in WinBUGS that subtracts the values of a MCMC vector for a parameter from another vector from different genotype/growing condition for comparison and generates a mean and probability distribution for significance testing.

3. RESULTS

3.1 Model Goodness-of-Fit

The MBLRC model performed well in predicting observed A_N across all growing environments including field ($R^2 = 0.87$, Figure 2a), growth chamber ($R^2 = 0.98$, Figure 2b), and greenhouse ($R^2 = 0.99$, Figure 2c) environments.

3.2 Effect of Growing Conditions on Phenotypic Expression of Photosynthesis

The probability distributions of the light response curve parameters for each genotype under different growing conditions (greenhouse (blue), field (green), and growth chamber (pink)) are shown in Figure 3. Across all three environmental conditions, α remains largely conserved. Across all three genotypes, α parameter for each environment shared parameter means and parameter space (overlapping posterior distributions), except one genotype (311795) where parameter (α) means are significantly different between greenhouse and growth chamber. Maximum photosynthesis rate (A_{max} , $\mu\text{mol m}^{-2} \text{s}^{-1}$) was consistently smallest in the highly controlled conditions (greenhouse), and greatest in the least controlled conditions (field) (Figure 3). None of the environments share parameter space for A_{max} and the parameter means are significantly different across growing conditions (Figure 3). Mitochondrial respiration (R_d , $\mu\text{mol m}^{-2} \text{s}^{-1}$) parameter estimates are not significantly different across environments in any genotype. While their parameter space partly overlapped, the lack of significant difference was likely due to the larger variability in parameter estimates of this parameter. Mean estimates of the shape parameter (θ) are greater in the growth chamber compared to the field but are only significantly different between growth chamber and field in 311795 (Figure 3j).

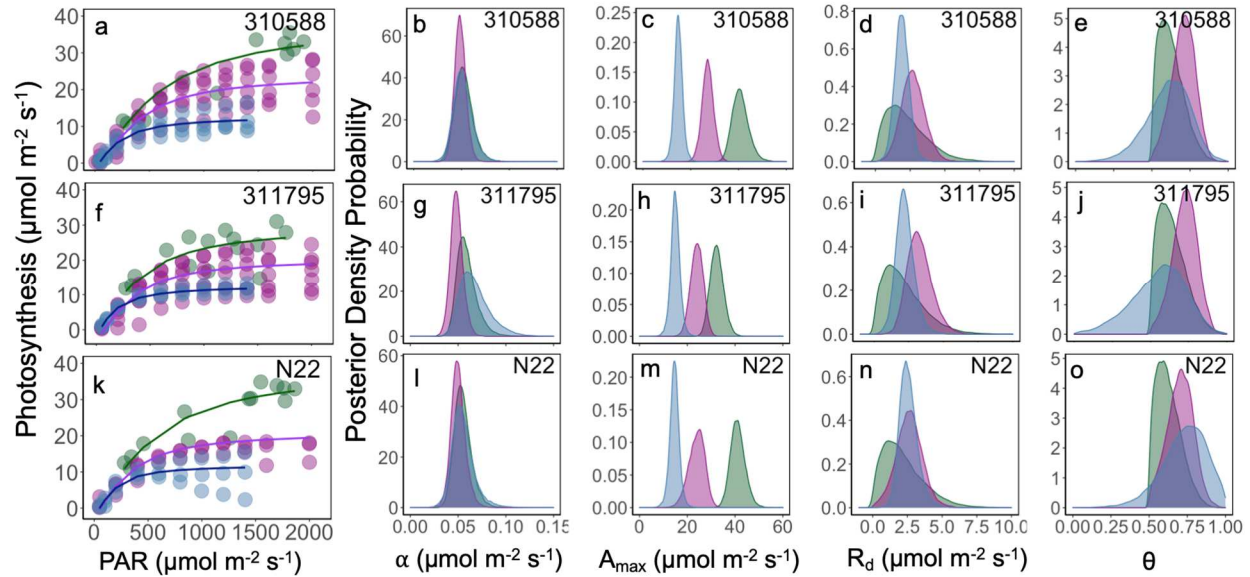


Figure 3. Photosynthesis light response curves (a, f, k) and posterior density distribution of photosynthesis model parameters α ($\mu\text{mol m}^{-2} \text{s}^{-1}$), A_{max} ($\mu\text{mol m}^{-2} \text{s}^{-1}$), R_d ($\mu\text{mol m}^{-2} \text{s}^{-1}$), and θ for three rice (*Oryza sativa*) genotypes under field (green), growth chamber (pink), and greenhouse (blue) conditions. Green, pink, and blue lines are the fit of a non-rectangular hyperbola model for field, growth chamber, and greenhouse plants, respectively.

3.3 Effect of Measurement Methods on Phenotypic Expression of Photosynthesis

Similar to growing conditions, α , R_d , and θ parameters were mostly similar across measurement methods, but A_{max} was significantly different across measurement methods (Figure 4). For example, α was significantly greater in the non-sequential method only in 310723 and ZHE, and R_d was significantly lower in the non-sequential method only in 310723. θ was not significantly different between methods across any genotype. Only A_{max} was significantly different between the sequential and non-sequential methods in all genotypes, except 311677 (Figure 4r).

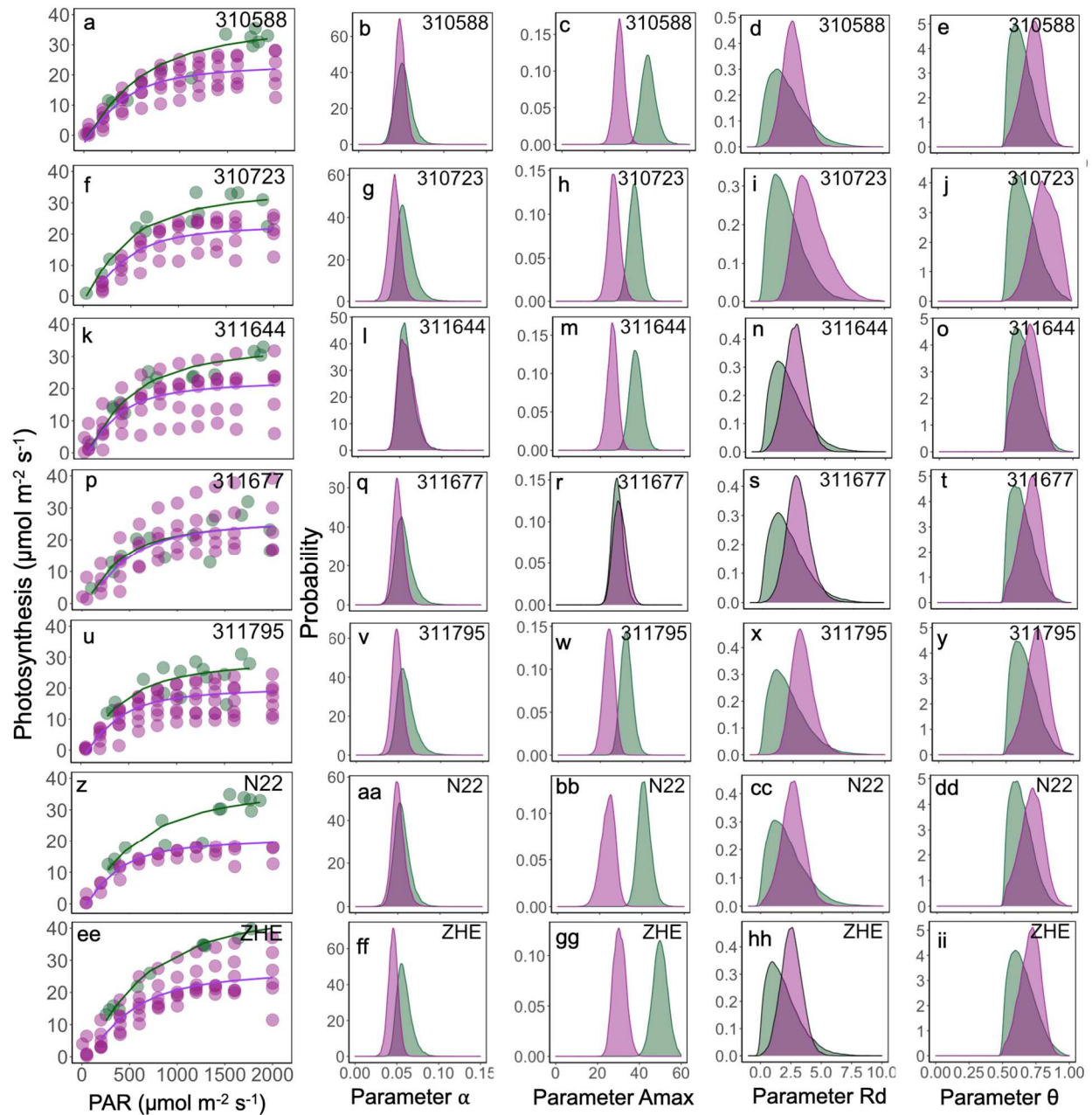


Figure 4. Photosynthetic light response curves (a, f, k, p) and photosynthetic model parameters α (b, g, l, q), A_{max} (c, h, m, r), R_d (d, i, n, s), and θ (e, j, o, t) for four rice (*Oryza sativa*) genotypes under field (green) and growth chamber (pink) conditions. Green and pink lines are the fit of a non-rectangular hyperbola model for field and growth chamber plants, respectively.

4. DISCUSSION

4.1 Effect of Growing Conditions on Phenotypic Expression of Photosynthesis

Light response curves play a vital role in understanding plant characteristics and quantifying photosynthetic acclimation under different conditions (Herrmann et al., 2019). Our results show that maximum photosynthesis rate (A_{max}) was greatest in the field plants across all genotypes (Figure 2, column 3). Plants acclimate to the environment they are in (Walters, 2005; Dyson et al., 2015; Herrmann et al., 2019), and it has been well documented that plants grown at higher light intensities, such as those outside in the field, have greater A_{max} than those at grown under lower light intensities, such as in a greenhouse (Ögren, 1993; Bailey et al., 2001; Walters, 2005; Perkins et al., 2006; Athanasiou et al., 2010; Du et al., 2020).

Research has also shown that plants that are grown at low light and are moved to high light will increase their photosynthetic capacity (Walters, 2005; Athanasiou et al., 2010). Our growth chamber plants, which were grown at lower light intensities ($600 \mu\text{mol m}^{-2} \text{s}^{-1}$), often had A_{max} values similar to field plants. The high variability seen in the light response curves of growth chamber plants, though, may indicate that some leaves may have been shaded and not fully acclimated to the new light intensity, and thus had lower maximum photosynthesis.

We expected a smaller shape parameter (θ) in field plants as θ is generally smaller in plants acclimated to high light (Ögren, 1993). Typically, θ ranges from 0.7 to 0.99 ($\theta = 1$ is a Blackman curve and $\theta = 0$ is a rectangular hyperbola (Evans et al., 1993; Ögren and Evans, 1993)). Ögren (1993) found that when grown under lower light, algal cells and willow (*Salix*) leaves had lower A_{max} and higher θ , a finding that was only partially consistent with our results. While our greenhouse plants had lower A_{max} compared with field and growth chamber plants, θ was only significantly different between the field and growth chamber for 311795.

While growth chamber plants had much greater variability in the light response curves, those at the top of their range were quite similar to the field curves. If allowed to acclimate outside for several days before measurements, photosynthesis measured in plants grown formerly in pots in controlled environments may be very similar to photosynthesis measured in field plants. Field curves were quite different from those conducted on greenhouse plants, but the smallest curves of the growth chamber plants were similar to those of the greenhouse plants. Our results captured a gradient of growing conditions and plasticity of rice genotypes acclimated to those conditions (Figure 4).

Photosynthesis model parameters are a critical piece of understanding the gene and environment interactions of different plant genotypes (Rascher et al., 2000). Photosynthetic parameters have been shown to differ between the field and lab experiments (Mishra et al., 2012; Tian-gen et al., 2017) and our results supported the previous studies showing these differences. Field plants experience a variety of light, temperature, and humidity that cannot be easily replicated in a greenhouse. Additionally, greenhouse-grown plants may not have the nutrition, soil depth, etc. to meet their own growth demands. Thus, the photosynthetic parameters and physiological characteristics obtained from greenhouse plants should not be taken as representative of field-grown plants (Tian-gen et al., 2017), but the growth chamber or greenhouse grown plants acclimated to field conditions before measurements may be used for pot experiments.

4.2 Effect of Measurement Methods on Phenotypic Expression of Photosynthesis

Our results show that the non-sequential survey method captured greater variability compared to sequential method. The non-sequential method resulted in a greater A_{max} across nearly every genotype surveyed (Figure 4), indicating that light response curves conducted

sequentially may underestimate maximum photosynthesis capacity of some genotypes. However, the two methods were very similar in their estimations of α , R_d , and θ , suggesting that the non-sequential method is a valid tool to use when phenotyping.

5. CONCLUSIONS

The light response curve is a useful tool for quantifying the phenotypic plasticity of plant photosynthesis. Our results highlight that the growing conditions have a significant effect on phenotypic expression of photosynthesis in rice genotypes, but different measurement methods produce similar results. We show that light response curve parameters generated for plants grown in lower light environments must not be assumed as characteristic of plants grown in field or high-light environments. Furthermore, different methods for generating response curves provide different information about the plant. There is a critical need to better understand the phenotypic plasticity of different genotypes, but care should be taken to ensure that the phenotyping environment and methodology are appropriate for the conclusions drawn.

6. REFERENCES

- Agrama, H. A., Yan, W., Lee, F., Fjellstrom, R., Chen, M.-H., Jia, M., et al. (2009). Genetic assessment of a mini-core subset developed from the USDA rice genebank. *Crop Science* 49, 1336–1346. doi:10.2135/cropsci2008.06.0551.
- Athanasίου, K., Dyson, B. C., Webster, R. E., and Johnson, G. N. (2010). Dynamic acclimation of photosynthesis increases plant fitness in changing environments. *Plant Physiol* 152, 366–373. doi:10.1104/pp.109.149351.
- Bailey, S., Walters, R. G., Jansson, S., and Horton, P. (2001). Acclimation of *Arabidopsis thaliana* to the light environment: the existence of separate low light and high light responses. *Planta* 213, 794–801. doi:10.1007/s004250100556.
- Battaglia, M., Beadle, C., and Loughhead, S. (1996). Photosynthetic temperature responses of *Eucalyptus globulus* and *Eucalyptus nitens*. *Tree Physiol* 16, 81–89.

doi:10.1093/treephys/16.1-2.81.

- Berry, J., and Bjorkman, O. (1980). Photosynthetic response and adaptation to temperature in higher plants. *Annual Review of Plant Physiology* 31, 491–543.
doi:10.1146/annurev.pp.31.060180.002423.
- Bouman, B. A. M., and Tuong, T. P. (2001). Field water management to save water and increase its productivity in irrigated lowland rice. *Agricultural Water Management* 49, 11–30.
doi:10.1016/S0378-3774(00)00128-1.
- Brooks, S. P., and Gelman, A. (1998). General Methods for Monitoring Convergence of Iterative Simulations. *Journal of Computational and Graphical Statistics* 7, 434–455.
doi:10.1080/10618600.1998.10474787.
- Clark, J. S., and Gelfand, A. (2006). *Hierarchical Modelling for the Environmental Sciences: Statistical Methods and Applications*. Oxford University Press Available at:
<https://www.semanticscholar.org/paper/Hierarchical-Modelling-for-the-Environmental-and-Clark-Gelfand/c83ec91c9ef0077c127c0c7aa7e0073bafa525e9> [Accessed November 24, 2021].
- Coe, R. A., and Lin, H. (2018). “Light-Response Curves in Land Plants,” in *Photosynthesis: Methods and Protocols Methods in Molecular Biology.*, ed. S. Covshoff (New York, NY: Springer), 83–94. doi:10.1007/978-1-4939-7786-4_5.
- Dreyer, E., Le Roux, X., Montpied, P., Daudet, F. A., and Masson, F. (2001). Temperature response of leaf photosynthetic capacity in seedlings from seven temperate tree species. *Tree Physiol* 21, 223–232. doi:10.1093/treephys/21.4.223.
- Du, T., Meng, P., Huang, J., Peng, S., and Xiong, D. (2020). Fast photosynthesis measurements for phenotyping photosynthetic capacity of rice. *Plant Methods* 16, 6.
doi:10.1186/s13007-020-0553-2.
- Dyson, B. C., Allwood, J. W., Feil, R., Xu, Y., Miller, M., Bowsher, C. G., et al. (2015). Acclimation of metabolism to light in *Arabidopsis thaliana*: the glucose 6-phosphate/phosphate translocator GPT2 directs metabolic acclimation. *Plant, Cell & Environment* 38, 1404–1417. doi:10.1111/pce.12495.
- Evans, J. R., Jakobsen, I., and Ogren, E. (1993). Photosynthetic light-response curves: 2. Gradients of light absorption and photosynthetic capacity. *Planta* 189.
doi:10.1007/BF00195076.
- Farquhar, G., von Caemmerer, S., and Berry, J. (1980). *A biochemical model of photosynthetic CO₂*. doi:10.1007/BF00386231.
- Gelman, A., Carlin, J. B., Stern, H. S., Dunson, D. B., Vehtari, A., and Rubin, D. B. (2021). *Bayesian Data Analysis*. 677.

- Herrmann, H. A., Schwartz, J.-M., and Johnson, G. N. (2019). From empirical to theoretical models of light response curves - linking photosynthetic and metabolic acclimation. *Photosynth Res.* doi:10.1007/s11120-019-00681-2.
- Houliiez, E., Lefebvre, S., Lizon, F., and Schmitt, F. G. (2017). Rapid light curves (RLC) or non-sequential steady-state light curves (N-SSLIC): which fluorescence-based light response curve methodology robustly characterizes phytoplankton photosynthetic activity and acclimation status? *Mar Biol* 164, 175. doi:10.1007/s00227-017-3208-8.
- Kumar, A. (2017). Development and characterization of rice genotypes for water use efficiency and drought resistance. *ProQuest Dissertations and Theses*. Available at: <https://www.proquest.com/docview/2317708251/abstract/CDE662A53F2C4753PQ/1> [Accessed October 30, 2021].
- LI-COR (2021). Light response curves. *LI-6800 Portable Photosynthesis System*. Available at: <https://www.licor.com/env/support/LI-6800/topics/light-response-curves.html> [Accessed November 16, 2021].
- Lobo, F. de A., de Barros, M. P., Dalmagro, H. J., Dalmolin, Â. C., Pereira, W. E., de Souza, É. C., et al. (2013). Fitting net photosynthetic light-response curves with Microsoft Excel — a critical look at the models. *Photosynthetica* 51, 445–456. doi:10.1007/s11099-013-0045-y.
- Lunn, D. J., Thomas, A., Best, N., and Spiegelhalter, D. (2000). WinBUGS - A Bayesian modelling framework: Concepts, structure, and extensibility. *Statistics and Computing* 10, 325–337.
- McDermitt, D. K., Norman, J. M., Davis, J. T., Ball, T. M., Arkebauer, T. J., Welles, J. M., et al. (1989). CO₂ response curves can be measured with a field-portable closed-loop photosynthesis system. *Annales des Sciences Forestières* 46, 416s–420s. doi:10.1051/forest:19890593.
- Medlyn, B. E., Dreyer, E., Ellsworth, D., Forstreuter, M., Harley, P. C., Kirschbaum, M. U. F., et al. (2002). Temperature response of parameters of a biochemically based model of photosynthesis. II. A review of experimental data. *Plant, Cell & Environment* 25, 1167–1179. doi:10.1046/j.1365-3040.2002.00891.x.
- Mishra, Y., Johansson Jänkänpää, H., Kiss, A. Z., Funk, C., Schröder, W. P., and Jansson, S. (2012). Arabidopsis plants grown in the field and climate chambers significantly differ in leaf morphology and photosystem components. *BMC Plant Biology* 12, 6. doi:10.1186/1471-2229-12-6.
- Mohanty, S., Wassmann, R., Nelson, A., Moya, P., and Jagadish, S. V. K. (2013). Rice and climate change: significance for food security and vulnerability. *IRRI Discussion Paper Series No. 49*, 18.

- Ögren, E. (1993). Convexity of the photosynthetic light-response curve in relation to intensity and direction of light during growth. *Plant Physiology* 101, 1013–1019. doi:10.1104/pp.101.3.1013.
- Ögren, E., and Evans, J. R. (1993). Photosynthetic light-response curves I. The influence of CO₂ partial pressure and leaf inversion. *Planta* 189, 182–190.
- Perkins, R. G., Mouget, J.-L., Lefebvre, S., and Lavaud, J. (2006). Light response curve methodology and possible implications in the application of chlorophyll fluorescence to benthic diatoms. *Mar Biol* 149, 703–712. doi:10.1007/s00227-005-0222-z.
- Pieruschka, R., and Schurr, U. (2019). Plant phenotyping: past, present, and future. *Plant Phenomics*. doi:10.34133/2019/7507131.
- Ralph, P. J., and Gademann, R. (2005). Rapid light curves: a powerful tool to assess photosynthetic activity. *Aquatic Botany* 82, 222–237. doi:10.1016/j.aquabot.2005.02.006.
- Rascher, U., Liebig, M., and Lüttge, U. (2000). Evaluation of instant light-response curves of chlorophyll fluorescence parameters obtained with a portable chlorophyll fluorometer on site in the field. *Plant, Cell & Environment* 23, 1397–1405. doi:10.1046/j.1365-3040.2000.00650.x.
- Robert, C. P., and Casella, G. *Introducing Monte Carlo Methods with R*. 239.
- Serôdio, J., Ezequiel, J., Frommlet, J., Laviale, M., and Lavaud, J. (2013). A method for the rapid generation of nonsequential light-response curves of chlorophyll fluorescence. *Plant Physiology* 163, 1089–1102. doi:10.1104/pp.113.225243.
- Sharkey, T. D., Bernacchi, C. J., Farquhar, G. D., and Singsaas, E. L. (2007). Fitting photosynthetic carbon dioxide response curves for C₃ leaves. *Plant, Cell & Environment* 30, 1035–1040. doi:10.1111/j.1365-3040.2007.01710.x.
- Sims, D. A., Luo, Y., and Seemann, J. R. (1998). Importance of leaf versus whole plant CO₂ environment for photosynthetic acclimation. *Plant, Cell & Environment* 21, 1189–1196. doi:10.1046/j.1365-3040.1998.00377.x.
- Sultan, S. E. (2000). Phenotypic plasticity for plant development, function and life history. *Trends in Plant Science* 5, 537–542. doi:10.1016/S1360-1385(00)01797-0.
- Thornley, J. (1998). Dynamic Model of Leaf Photosynthesis with Acclimation to Light and Nitrogen. *Annals of Botany* 81, 421–430. doi:10.1006/anbo.1997.0575.
- Thornley, J. H. M., and Johnson, I. R. (1990). *Plant and Crop Modeling*. Oxford: University Press.
- Tian-gen, C., Chang-peng, X., Ming-nan, Q., Hong-long, Z., Qing-feng, S., and Xin-guang, Z.

(2017). Evaluation of protocols for measuring leaf photosynthetic properties of field-grown rice. *Rice Science* 24, 1–9. doi:10.1016/j.rsci.2016.08.007.

USDA Web Soil Survey. Available at:

<https://websoilsurvey.sc.egov.usda.gov/App/WebSoilSurvey.aspx> [Accessed November 10, 2021].

Wagner, S. W., and Reicosky, D. C. (1992). Closed-chamber effects on leaf temperature, canopy photosynthesis, and evapotranspiration. *Agronomy Journal* 84, 731–738. doi:10.2134/agronj1992.00021962008400040035x.

Walters, R. G. (2005). Towards an understanding of photosynthetic acclimation. *J Exp Bot* 56, 435–447. doi:10.1093/jxb/eri060.

Wikle, C. K. (2003). Hierarchical Models in Environmental Science. *International Statistical Review* 71, 181–199. doi:10.1111/j.1751-5823.2003.tb00192.x.

Zelitch, I. (1982). The close relationship between net photosynthesis and crop yield. *BioScience* 32, 796–802. doi:10.2307/1308973.

APPENDIX 1

Table A1. Summary statistics for genotype-level parameters in field including A_{max} (maximum rate of photosynthesis), Rd (mitochondrial respiration), α (apparent quantum efficiency of photosynthesis), and θ (curvature shape parameter). [1] = 310588, [2] = 310723, [3] = 311644, [4] = 311677, [5] = 311795, [6] = Nagina 22, [7] = Zhe733. D is the sum of the squared deviation and SD is the standard deviation of modeled observations.

Node	Mean	SD	2.50%	Median	97.50%	Sample
D	2669.0000	411.9000	1957.0000	2638.0000	3565.0000	29985
sig.obs	3.6880	0.2864	3.1790	3.6710	4.2980	29985
Genotype-level parameters						
sig. A_{max}	7.2740	1.5640	4.2090	7.3350	9.8330	29985
sig.Rd	0.7548	0.7046	0.0230	0.5540	2.6620	29985
sig.alpha	0.0072	0.0065	0.0003	0.0056	0.0235	29985
sig.theta	0.0587	0.0560	0.0019	0.0438	0.1965	29985
Amax[1]	40.8200	3.4720	34.7900	40.5800	48.3900	29985
Amax[2]	37.5700	2.9750	31.9800	37.4900	43.6500	29985
Amax[3]	37.0400	3.0660	31.3200	36.9300	43.3800	29985
Amax[4]	29.3000	2.6870	24.4400	29.1500	35.0100	29985
Amax[5]	32.3900	2.7980	27.2700	32.2700	38.2500	29985
Amax[6]	41.1300	3.0860	35.5000	40.9700	47.6200	29985
Amax[7]	49.9900	3.5000	43.2400	49.9400	56.9500	29985
Rd[1]	2.2520	1.4790	0.2169	1.9810	5.7990	29985
Rd[2]	2.0250	1.3650	0.1673	1.7720	5.2870	29985
Rd[3]	2.0850	1.4070	0.1869	1.8120	5.4700	29985

Table A1 Continued

Node	Mean	SD	2.50%	Median	97.50%	Sample
Rd[5]	2.1420	1.4820	0.1814	1.8480	5.7540	29985
Rd[6]	2.2050	1.5040	0.1927	1.9060	5.8110	29985
Rd[7]	1.9290	1.3620	0.1393	1.6540	5.2220	29985
alpha[1]	0.0524	0.0095	0.0357	0.0518	0.0733	29985
alpha[2]	0.0600	0.0102	0.0445	0.0584	0.0842	29985
alpha[3]	0.0580	0.0095	0.0431	0.0567	0.0801	29985
alpha[4]	0.0578	0.0106	0.0409	0.0564	0.0826	29985
alpha[5]	0.0592	0.0107	0.0430	0.0576	0.0845	29985
alpha[6]	0.0549	0.0091	0.0393	0.0540	0.0755	29985
alpha[7]	0.0587	0.0086	0.0451	0.0576	0.0786	29985
theta[1]	0.6255	0.0803	0.5101	0.6135	0.8093	29985
theta[2]	0.6519	0.0965	0.5137	0.6357	0.8751	29985
theta[3]	0.6352	0.0853	0.5119	0.6226	0.8280	29985
theta[4]	0.6339	0.0862	0.5107	0.6206	0.8319	29985
theta[5]	0.6408	0.0905	0.5118	0.6265	0.8494	29985
theta[6]	0.6267	0.0801	0.5099	0.6151	0.8086	29985
theta[7]	0.6526	0.0946	0.5150	0.6383	0.8676	29985

Table A2. Summary statistics for plant-level and genotype-level parameters in growth chamber including A_{max} (maximum rate of photosynthesis), Rd (mitochondrial respiration), α (apparent quantum efficiency of photosynthesis), and θ (curvature shape parameter). [1] = 310588, [2] = 310723, [3] = 311644, [4] = 311677, [5] = 311795, [6] = Nagina 22, [7] = Zhe733. D is the sum of the squared deviation and SD is the standard deviation of modeled observations.

Node	Mean	SD	2.50%	Median	97.50%	Sample
D	1298.0000	139.9000	1043.0000	1291.0000	1589.0000	29991
sig.obs	1.3320	0.0720	1.1960	1.3300	1.4770	29991
Genotype level parameters						
sig.Amax	6.8850	0.9791	5.1710	6.8030	9.0210	29991
sig.Rd	1.9010	0.5556	0.9148	1.8680	3.0850	29991
sig.alpha	0.0124	0.0029	0.0073	0.0122	0.0186	29991
sig.theta	0.0975	0.0560	0.0060	0.0980	0.2092	29991
mu.Amax[1]	27.1600	2.4650	22.2700	27.1200	32.1100	29991
mu.Amax[2]	27.7500	2.8380	22.3600	27.6500	33.6200	29991
mu.Amax[3]	25.6600	2.5000	20.5300	25.7300	30.4100	29991
mu.Amax[4]	30.3600	3.1100	24.7600	30.2000	36.7100	29991
mu.Amax[5]	24.0400	2.6220	18.7700	24.0800	28.9900	29991
mu.Amax[6]	23.9100	3.3590	16.8200	24.1600	29.8700	29991
mu.Amax[7]	30.5400	2.9870	25.1200	30.4500	36.6100	29991
mu.Rd[1]	2.7090	0.8454	1.1170	2.6800	4.4420	29991
mu.Rd[2]	4.0500	1.3930	1.9920	3.8040	7.3360	29991
mu.Rd[3]	2.5850	0.8913	0.8731	2.5750	4.3860	29991
mu.Rd[4]	2.9850	0.9799	1.2090	2.9240	5.1120	29991
mu.Rd[5]	3.2890	0.8972	1.7430	3.2110	5.2550	29991
mu.Rd[6]	2.6350	0.9423	0.7572	2.6340	4.5180	29991

Table A2 Continued

Node	Mean	SD	2.50%	Median	97.50%	Sample
mu.Rd[7]	2.5520	0.8608	0.9190	2.5360	4.2840	29991
mu.alpha[1]	0.0487	0.0060	0.0372	0.0485	0.0609	29991
mu.alpha[2]	0.0467	0.0073	0.0327	0.0466	0.0620	29991
mu.alpha[3]	0.0582	0.0096	0.0428	0.0571	0.0792	29991
mu.alpha[4]	0.0508	0.0065	0.0389	0.0504	0.0648	29991
mu.alpha[5]	0.0485	0.0066	0.0363	0.0482	0.0624	29991
mu.alpha[6]	0.0503	0.0076	0.0365	0.0497	0.0668	29991
mu.alpha[7]	0.0456	0.0057	0.0342	0.0457	0.0569	29991
mu.theta[1]	0.7058	0.0763	0.5481	0.7094	0.8465	29991
mu.theta[2]	0.7927	0.0916	0.6081	0.7938	0.9533	29991
mu.theta[3]	0.6675	0.0782	0.5181	0.6709	0.8111	29991
mu.theta[4]	0.6961	0.0782	0.5338	0.7006	0.8372	29991
mu.theta[5]	0.7249	0.0801	0.5567	0.7283	0.8748	29991
mu.theta[6]	0.7033	0.0848	0.5318	0.7064	0.8645	29991
mu.theta[7]	0.7073	0.0771	0.5462	0.7119	0.8460	29991
Plant level parameters						
Amax[1]	27.9900	2.4760	23.1900	27.9800	32.8600	29991
Amax[2]	29.7900	1.8870	26.1700	29.7700	33.6400	29991
Amax[3]	20.1800	1.3640	17.7000	20.1200	23.0200	29991
Amax[4]	34.7300	2.3830	30.2300	34.6500	39.6100	29991
Amax[5]	31.5600	1.6380	28.5200	31.4700	34.9800	29991

Table A2 Continued

Node	Mean	SD	2.50%	Median	97.50%	Sample
Amax[8]	20.4700	2.3840	15.9900	20.4200	25.3200	29991
Amax[9]	33.2400	2.6680	28.2700	33.1800	38.6500	29991
Amax[10]	29.7400	2.7110	25.1100	29.5100	35.5000	29991
Amax[11]	26.8600	2.5670	22.0700	26.7800	32.1000	29991
Amax[12]	30.2400	2.2090	26.0800	30.1700	34.7000	29991
Amax[13]	18.2200	1.4460	15.5500	18.1600	21.1600	29991
Amax[14]	26.7400	1.3520	24.2500	26.6800	29.5700	29991
Amax[15]	26.8400	1.6630	23.7200	26.7900	30.2300	29991
Amax[16]	33.2800	1.2430	30.9700	33.2300	35.8800	29991
Amax[17]	13.6300	2.2130	9.5430	13.5500	18.1500	29991
Amax[18]	24.0800	2.2030	19.9400	24.0300	28.5300	29991
Amax[19]	29.6800	1.6880	26.5300	29.6300	33.1400	29991
Amax[20]	37.2600	2.8250	31.9100	37.1900	42.9300	29991
Amax[21]	44.2800	2.0430	40.6300	44.1700	48.6000	29991
Amax[22]	28.0400	3.3600	21.8600	27.9600	34.7600	29991
Amax[23]	25.4300	1.9280	21.8000	25.3700	29.3700	29991
Amax[24]	26.5900	1.8170	23.1700	26.5200	30.3000	29991
Amax[25]	20.3400	1.4330	17.7000	20.2800	23.2900	29991
Amax[26]	20.0500	2.1090	16.1400	20.0000	24.3700	29991
Amax[27]	29.9500	1.9340	26.3300	29.8900	33.9200	29991
Amax[28]	16.0300	1.4530	13.3000	15.9800	18.9600	29991
Amax[29]	18.4100	2.6670	13.5600	18.2800	23.9600	29991

Table A2 Continued

Node	Mean	SD	2.50%	Median	97.50%	Sample
Amax[30]	22.4600	1.5470	19.5600	22.4200	25.5800	29991
Amax[31]	20.9400	1.3990	18.4300	20.8600	23.8700	29991
Amax[32]	18.5700	1.5650	15.5900	18.5400	21.7100	29991
Amax[33]	29.1800	2.6930	24.3700	29.0100	34.9800	29991
Amax[34]	29.9400	2.3730	25.4700	29.9000	34.6900	29991
Amax[35]	30.9900	2.1550	27.1800	30.8600	35.6000	29991
Amax[36]	40.1600	2.8290	34.8600	40.0800	45.9600	29991
Amax[37]	41.7600	2.0880	38.0000	41.6200	46.2300	29991
Amax[38]	24.0000	2.4220	20.0300	23.8400	28.8200	29991
Rd[1]	4.7520	1.7730	1.5440	4.6810	8.4030	29991
Rd[2]	2.6280	1.0980	0.5787	2.5950	4.8540	29991
Rd[3]	1.5910	0.9373	0.1241	1.5040	3.6500	29991
Rd[4]	2.7870	1.4340	0.3551	2.6760	5.8660	29991
Rd[5]	0.7884	0.5749	0.0322	0.6795	2.1330	29991
Rd[6]	2.5440	1.2010	0.4029	2.4710	5.0530	29991
Rd[7]	4.3180	1.7510	1.1460	4.2170	7.9920	29991
Rd[8]	5.2730	1.9910	1.7320	5.1510	9.4590	29991
Rd[9]	4.1070	1.7330	0.9729	4.0040	7.7430	29991
Rd[10]	4.8970	1.7840	1.7220	4.7830	8.6470	29991
Rd[11]	5.6060	1.8920	2.2110	5.5070	9.5770	29991
Rd[12]	3.2980	1.6420	0.4796	3.1720	6.8030	29991
Rd[13]	2.4090	1.1340	0.3592	2.3550	4.7580	29991

Table A2 Continued

Node	Mean	SD	2.50%	Median	97.50%	Sample
Rd[14]	0.9011	0.6199	0.0454	0.8000	2.3240	29991
Rd[15]	2.1840	1.1190	0.2663	2.1110	4.5540	29991
Rd[16]	0.1807	0.1740	0.0044	0.1294	0.6400	29991
Rd[17]	4.9470	1.9410	1.3650	4.8820	8.8910	29991
Rd[18]	4.2590	1.8060	1.0230	4.1700	8.0120	29991
Rd[19]	1.9400	1.0340	0.2035	1.8660	4.1330	29991
Rd[20]	3.1930	1.5390	0.5173	3.0930	6.4810	29991
Rd[21]	0.2622	0.2469	0.0067	0.1890	0.9040	29991
Rd[22]	5.7280	2.3690	1.6060	5.5420	10.8300	29991
Rd[23]	3.4110	1.5200	0.6510	3.3300	6.6240	29991
Rd[24]	2.4620	1.0980	0.4371	2.4290	4.6890	29991
Rd[25]	2.1710	1.0670	0.2889	2.1290	4.4050	29991
Rd[26]	5.2060	1.7920	2.0020	5.1180	8.9980	29991
Rd[27]	2.6290	1.1100	0.5602	2.5900	4.8990	29991
Rd[28]	2.9010	1.1260	0.7601	2.8770	5.1790	29991
Rd[29]	5.8830	2.3450	1.8520	5.6860	10.9000	29991
Rd[30]	2.3540	1.1030	0.3640	2.3020	4.6580	29991
Rd[31]	1.3400	0.8810	0.0718	1.2160	3.3200	29991
Rd[32]	2.7640	1.1450	0.6268	2.7320	5.1030	29991
Rd[33]	2.1610	1.0660	0.3167	2.1000	4.4190	29991
Rd[34]	3.7720	1.6310	0.8632	3.6810	7.1850	29991
Rd[35]	1.5870	0.9447	0.1267	1.4910	3.6700	29991

Table A2 Continued

Node	Mean	SD	2.50%	Median	97.50%	Sample
Rd[36]	2.8200	1.4450	0.3831	2.7060	5.9140	29991
Rd[37]	0.2415	0.2293	0.0063	0.1738	0.8449	29991
Rd[38]	2.7900	1.1860	0.6481	2.7260	5.2620	29991
alpha[1]	0.0436	0.0088	0.0289	0.0429	0.0629	29991
alpha[2]	0.0512	0.0079	0.0376	0.0505	0.0684	29991
alpha[3]	0.0553	0.0098	0.0385	0.0544	0.0767	29991
alpha[4]	0.0483	0.0076	0.0357	0.0476	0.0650	29991
alpha[5]	0.0554	0.0069	0.0436	0.0548	0.0707	29991
alpha[6]	0.0347	0.0096	0.0198	0.0334	0.0569	29991
alpha[7]	0.0519	0.0094	0.0368	0.0508	0.0729	29991
alpha[8]	0.0377	0.0115	0.0197	0.0363	0.0636	29991
alpha[9]	0.0478	0.0088	0.0337	0.0468	0.0676	29991
alpha[10]	0.0433	0.0090	0.0301	0.0418	0.0644	29991
alpha[11]	0.0437	0.0095	0.0285	0.0424	0.0653	29991
alpha[12]	0.0559	0.0107	0.0382	0.0549	0.0796	29991
alpha[13]	0.0596	0.0126	0.0376	0.0586	0.0867	29991
alpha[14]	0.0632	0.0092	0.0474	0.0624	0.0834	29991
alpha[15]	0.0589	0.0105	0.0415	0.0579	0.0823	29991
alpha[16]	0.0869	0.0104	0.0688	0.0860	0.1099	29991
alpha[17]	0.0523	0.0153	0.0244	0.0519	0.0833	29991
alpha[18]	0.0451	0.0106	0.0275	0.0442	0.0681	29991
alpha[19]	0.0550	0.0083	0.0411	0.0542	0.0733	29991

Table A2 Continued

Node	Mean	SD	2.50%	Median	97.50%	Sample
alpha[20]	0.0514	0.0079	0.0380	0.0506	0.0689	29991
alpha[21]	0.0677	0.0066	0.0563	0.0672	0.0818	29991
alpha[22]	0.0378	0.0096	0.0233	0.0365	0.0595	29991
alpha[23]	0.0495	0.0094	0.0335	0.0486	0.0700	29991
alpha[24]	0.0548	0.0090	0.0394	0.0541	0.0745	29991
alpha[25]	0.0576	0.0103	0.0399	0.0566	0.0805	29991
alpha[26]	0.0461	0.0103	0.0286	0.0453	0.0684	29991
alpha[27]	0.0502	0.0080	0.0365	0.0495	0.0679	29991
alpha[28]	0.0457	0.0109	0.0273	0.0448	0.0695	29991
alpha[29]	0.0320	0.0113	0.0149	0.0304	0.0578	29991
alpha[30]	0.0544	0.0100	0.0375	0.0536	0.0763	29991
alpha[31]	0.0520	0.0097	0.0358	0.0511	0.0736	29991
alpha[32]	0.0459	0.0108	0.0274	0.0451	0.0693	29991
alpha[33]	0.0300	0.0055	0.0216	0.0293	0.0427	29991
alpha[34]	0.0441	0.0081	0.0305	0.0433	0.0618	29991
alpha[35]	0.0447	0.0070	0.0333	0.0439	0.0602	29991
alpha[36]	0.0454	0.0065	0.0348	0.0447	0.0601	29991
alpha[37]	0.0600	0.0058	0.0500	0.0596	0.0724	29991
alpha[38]	0.0343	0.0092	0.0216	0.0329	0.0541	29991
theta[1]	0.7563	0.1173	0.5125	0.7607	0.9608	29991
theta[2]	0.7207	0.1105	0.4761	0.7296	0.9125	29991
theta[3]	0.6891	0.1169	0.4274	0.6996	0.8847	29991

Table A2 Continued

Node	Mean	SD	2.50%	Median	97.50%	Sample
theta[4]	0.6941	0.1110	0.4441	0.7051	0.8798	29991
theta[5]	0.7057	0.1095	0.4628	0.7154	0.8926	29991
theta[6]	0.6422	0.1362	0.3177	0.6611	0.8580	29991
theta[7]	0.8545	0.0913	0.6373	0.8725	0.9789	29991
theta[8]	0.7466	0.1389	0.4264	0.7648	0.9559	29991
theta[9]	0.8087	0.1031	0.5672	0.8244	0.9583	29991
theta[10]	0.8978	0.0895	0.6667	0.9239	0.9960	29991
theta[11]	0.8165	0.1115	0.5514	0.8341	0.9748	29991
theta[12]	0.6806	0.1183	0.4358	0.6846	0.8980	29991
theta[13]	0.6611	0.1209	0.4023	0.6670	0.8806	29991
theta[14]	0.6348	0.1181	0.3744	0.6445	0.8369	29991
theta[15]	0.6397	0.1196	0.3715	0.6486	0.8483	29991
theta[16]	0.6279	0.1111	0.3796	0.6376	0.8152	29991
theta[17]	0.6441	0.1284	0.3618	0.6521	0.8722	29991
theta[18]	0.6582	0.1229	0.3840	0.6693	0.8669	29991
theta[19]	0.6531	0.1158	0.3945	0.6643	0.8461	29991
theta[20]	0.7030	0.1115	0.4684	0.7098	0.9003	29991
theta[21]	0.6416	0.1115	0.3857	0.6534	0.8216	29991
theta[22]	0.8019	0.1469	0.5181	0.8074	0.9961	29991
theta[23]	0.7189	0.1155	0.4568	0.7312	0.9082	29991
theta[24]	0.7502	0.1113	0.5042	0.7599	0.9345	29991
theta[25]	0.7440	0.1120	0.4963	0.7538	0.9326	29991

Table A2 Continued

Node	Mean	SD	2.50%	Median	97.50%	Sample
theta[26]	0.7623	0.1221	0.4971	0.7713	0.9686	29991
theta[27]	0.7194	0.1125	0.4654	0.7318	0.9016	29991
theta[28]	0.7006	0.1276	0.4097	0.7150	0.9086	29991
theta[29]	0.6843	0.1374	0.3665	0.7009	0.9065	29991
theta[30]	0.6935	0.1181	0.4363	0.7035	0.8948	29991
theta[31]	0.6720	0.1255	0.3918	0.6832	0.8816	29991
theta[32]	0.7186	0.1303	0.4456	0.7239	0.9559	29991
theta[33]	0.6733	0.1272	0.3821	0.6857	0.8891	29991
theta[34]	0.7040	0.1139	0.4574	0.7124	0.8999	29991
theta[35]	0.6265	0.1280	0.3256	0.6443	0.8284	29991
theta[36]	0.7087	0.1056	0.4804	0.7172	0.8891	29991
theta[37]	0.6764	0.1088	0.4309	0.6872	0.8563	29991
theta[38]	0.8446	0.1425	0.5496	0.8843	0.9986	29991

Table A3. Summary statistics for plant-level and genotype-level parameters in greenhouse including A_{max} (maximum rate of photosynthesis), Rd (mitochondrial respiration), α (apparent quantum efficiency of photosynthesis), and θ (curvature shape parameter). [1] = 310588, [2] = 310723, [3] = 311644, [4] = 311677, [5] = 311795, [6] = Nagina 22, [7] = Zhe733. D is the sum of the squared deviation and SD is the standard deviation of modeled observations.

Node	Mean	SD	2.50%	Median	97.50%	Sample
D	41.75	9.596	26.83	40.49	64.21	29991
sig.obs	0.49	0.056	0.40	0.49	0.62	29991

Genotype-level parameters

Table A3 Continued

Node	Mean	SD	2.50%	Median	97.50%	Sample
sig.Amax	4.07	1.257	2.32	3.83	7.28	29991
sig.Rd	0.51	0.396	0.02	0.43	1.48	29991
sig.alpha	0.01	0.007	0.00	0.01	0.03	29991
sig.theta	0.24	0.106	0.07	0.22	0.49	29991
mu.Amax[1]	14.83	1.825	11.20	14.80	18.57	29991
mu.Amax[2]	15.00	1.976	11.08	14.96	19.05	29991
mu.Amax[3]	14.62	1.986	10.61	14.63	18.60	29991
mu.Rd[1]	1.91	0.522	0.92	1.90	2.97	29991
mu.Rd[2]	2.23	0.668	1.03	2.19	3.71	29991
mu.Rd[3]	2.58	0.658	1.48	2.52	4.06	29991
mu.alpha[1]	0.05	0.010	0.03	0.05	0.07	29991
mu.alpha[2]	0.07	0.016	0.04	0.06	0.11	29991
mu.alpha[3]	0.05	0.012	0.04	0.05	0.08	29991
mu.theta[1]	0.61	0.143	0.30	0.62	0.86	29991
mu.theta[2]	0.56	0.174	0.18	0.57	0.86	29991
mu.theta[3]	0.73	0.147	0.40	0.74	0.97	29991

Plant-level parameters

node	mean	sd	error	0.03	median	start
Amax[1]	12.59	0.827	10.92	12.61	14.15	29991

Table A3 Continued

Node	Mean	SD	2.50%	Median	97.50%	Sample
Amax[4]	13.03	0.778	11.55	13.02	14.60	29991
Amax[5]	17.19	1.045	15.25	17.15	19.32	29991
Amax[6]	15.00	0.905	13.30	14.98	16.82	29991
Amax[7]	13.54	0.863	11.89	13.52	15.28	29991
Amax[8]	18.55	1.001	16.69	18.51	20.60	29991
Amax[9]	12.67	0.869	11.23	12.58	14.66	29991
Amax[10]	11.85	1.266	9.91	11.67	14.75	29991
Rd[1]	1.66	0.611	0.40	1.67	2.84	29991
Rd[2]	1.80	0.590	0.65	1.79	2.99	29991
Rd[3]	2.05	0.536	1.07	2.03	3.19	29991
Rd[4]	1.93	0.574	0.86	1.90	3.14	29991
Rd[5]	2.34	0.708	1.11	2.28	3.91	29991
Rd[6]	2.25	0.699	0.99	2.20	3.78	29991
Rd[7]	2.10	0.702	0.79	2.07	3.61	29991
Rd[8]	2.29	0.653	1.08	2.27	3.67	29991
Rd[9]	2.61	0.647	1.51	2.55	4.06	29991
Rd[10]	3.05	0.886	1.68	2.92	5.12	29991
alpha[1]	0.04	0.010	0.02	0.04	0.06	29991
alpha[2]	0.06	0.012	0.04	0.06	0.09	29991

Table A3 Continued

Node	Mean	SD	2.50%	Median	97.50%	Sample
alpha[5]	0.07	0.015	0.04	0.06	0.10	29991
alpha[6]	0.07	0.016	0.05	0.07	0.11	29991
alpha[7]	0.07	0.017	0.05	0.07	0.11	29991
alpha[8]	0.06	0.011	0.05	0.06	0.09	29991
alpha[9]	0.05	0.012	0.04	0.05	0.08	29991
alpha[10]	0.04	0.011	0.03	0.04	0.07	29991
theta[1]	0.35	0.197	0.02	0.35	0.73	29991
theta[2]	0.86	0.112	0.56	0.89	0.99	29991
theta[3]	0.58	0.170	0.19	0.61	0.85	29991
theta[4]	0.58	0.172	0.18	0.60	0.85	29991
theta[5]	0.55	0.181	0.14	0.58	0.84	29991
theta[6]	0.50	0.184	0.10	0.52	0.80	29991
theta[7]	0.51	0.185	0.11	0.53	0.82	29991
theta[8]	0.62	0.146	0.27	0.64	0.84	29991
theta[9]	0.88	0.105	0.60	0.91	0.99	29991
theta[10]	0.89	0.140	0.48	0.94	1.00	29991

CONCLUSION

Anthropogenic greenhouse gas emissions are increasing in concentration in the atmosphere, warming the climate and resulting in altered weather patterns across the globe. Data-driven solutions are needed to address the climatic threats to agriculture and global food security. In this research, we investigate current and develop new data analytics tools to support sustainable agriculture.

The focus of Chapter 1 was focused on developing a data analytics method to evaluate greenhouse gas emission disclosure and goal-setting from food and beverage companies. Agriculture and food production accounts for roughly a quarter of global emissions, and large companies have the influence and responsibility to reduce their overall emissions. We assessed the emission disclosure and climate goals of 100 companies and found that there has been an increase in recent years in companies disclosing their emissions and setting climate goals, but many of the goals lack the boldness required to significantly reduce global emissions enough to keep climate warming well below 2 °C. Our results highlight an urgent need to begin and continue to set truly ambitious, science-aligned climate goals.

The changing climate will increase drought concerns in agricultural production regions around the world, so in Chapter 2, we developed and tested a novel two-parameter mechanistic model to phenotype rice genotypes for drought sensitivity. Our results showed that there was a good agreement between the model predictions and the observed data. We used the PLA_{50} parameter to classify eight rice genotypes along a gradient of drought sensitivity, and our results were supported by the findings by others as well. This model, and the PLA_{50} parameter in particular, may provide a valuable tool to improve prediction of yield under environments of increased stress in future crop models.

In the final chapter, we dove deeper into plant phenotyping, and the current data analytics method for phenotyping, and compared two methods of generating light response curves on rice plants. The photosynthesis light response curve is a useful tool to phenotype plant photosynthesis capacity under a range of light conditions, and it can be used to understand plant plasticity and gene x environment interactions within a plant. We found that growing conditions significantly affect maximum photosynthesis, and that field environments, or pots in full-sun, would provide the most accurate interpretation of the plant's characteristics in real-life situations. Plants grown in controlled, lower-light environments should not be used to inform ideas about plants grown under full-sun environments. Plant plasticity means that phenotyping needs to occur in a range of environmental conditions, and care should be taken to ensure that the environment and phenotyping methodology are appropriate for the conclusions drawn about the plant.

The world's climate is rapidly changing, and there must be solutions to address the rising concerns that are innovative and based in science. This research aimed to provide science-based and data-derived tools to drive solutions towards slowing climate change and adapting to an uncertain future.

APPENDIX 2



J. William Fulbright College of Arts and Sciences
Department of Biological Sciences

Chapter 1, “Evaluating greenhouse gas emissions and climate mitigation goals of the global food and beverage sector” of Megan Reavis’s dissertation is accepted for publication in the journal *Frontiers in Sustainable Food Systems* in 2021 with co-authors, Jenny Ahlen, Joe Rudek, and Kusum Naithani.

I, Dr. Kusum Naithani, advisor of Megan Reavis, confirm Megan Reavis is the first author and completed at least 51% of the work for this manuscript.

Kusum Naithani
Associate Professor
University of Arkansas
Department of Biological Sciences

December 9, 2021

Date